NASA/CR—2002-211895 ARL–CR–0511

New Geometry of Worm Face Gear Drives With Conical and Cylindrical Worms: Generation, Simulation of Meshing, and Stress Analysis

Faydor L. Litvin, Alessandro Nava, Qi Fan, and Alfonso Fuentes
University of Illinois at Chicago, Chicago, Illinois

November 2002

The NASA STI Program Office . . . in Profile

Since its founding, NASA has been dedicated to the advancement of aeronautics and space science. The NASA Scientific and Technical Information (STI) Program Office plays a key part in helping NASA maintain this important role.

The NASA STI Program Office is operated by Langley Research Center, the Lead Center for NASA's scientific and technical information. The NASA STI Program Office provides access to the NASA STI Database, the largest collection of aeronautical and space science STI in the world. The Program Office is also NASA's institutional mechanism for disseminating the results of its research and development activities. These results are published by NASA in the NASA STI Report Series, which includes the following report types:

- TECHNICAL PUBLICATION. Reports of completed research or a major significant phase of research that present the results of NASA programs and include extensive data or theoretical analysis. Includes compilations of significant scientific and technical data and information deemed to be of continuing reference value. NASA's counterpart of peer-reviewed formal professional papers but has less stringent limitations on manuscript length and extent of graphic presentations.

- TECHNICAL MEMORANDUM. Scientific and technical findings that are preliminary or of specialized interest, e.g., quick release reports, working papers, and bibliographies that contain minimal annotation. Does not contain extensive analysis.

- CONTRACTOR REPORT. Scientific and technical findings by NASA-sponsored contractors and grantees.

- CONFERENCE PUBLICATION. Collected papers from scientific and technical conferences, symposia, seminars, or other meetings sponsored or cosponsored by NASA.

- SPECIAL PUBLICATION. Scientific, technical, or historical information from NASA programs, projects, and missions, often concerned with subjects having substantial public interest.

- TECHNICAL TRANSLATION. English-language translations of foreign scientific and technical material pertinent to NASA's mission.

Specialized services that complement the STI Program Office's diverse offerings include creating custom thesauri, building customized databases, organizing and publishing research results . . . even providing videos.

For more information about the NASA STI Program Office, see the following:

- Access the NASA STI Program Home Page at *http://www.sti.nasa.gov*

- E-mail your question via the Internet to help@sti.nasa.gov

- Fax your question to the NASA Access Help Desk at 301–621–0134

- Telephone the NASA Access Help Desk at 301–621–0390

- Write to:
  NASA Access Help Desk
  NASA Center for AeroSpace Information
  7121 Standard Drive
  Hanover, MD 21076

NASA/CR—2002-211895 ARL–CR–0511

New Geometry of Worm Face Gear Drives With Conical and Cylindrical Worms: Generation, Simulation of Meshing, and Stress Analysis

Faydor L. Litvin, Alessandro Nava, Qi Fan, and Alfonso Fuentes
University of Illinois at Chicago, Chicago, Illinois

Prepared under Grant NAG3–2450

National Aeronautics and
Space Administration

Glenn Research Center

November 2002

Acknowledgments

The authors express their deep gratitude to the Army Research Laboratory, NASA Glenn Research Center, and the Gleason Foundation for the financial support of this research project.

Available from

NASA Center for Aerospace Information
7121 Standard Drive
Hanover, MD 21076

National Technical Information Service
5285 Port Royal Road
Springfield, VA 22100

Available electronically at http://gltrs.grc.nasa.gov

New Geometry of Worm Face Gear Drives With Conical and Cylindrical Worms: Generation, Simulation of Meshing, and Stress Analysis

Faydor L. Litvin, Alessandro Nava, Qi Fan, and Alfonso Fuentes
University of Illinois at Chicago
Chicago, Illinois 60607

Abstract

New geometry of face worm gear drives with conical and cylindrical worms is proposed. The generation of the face worm-gear is based on application of a tilted head-cutter (grinding tool) instead of application of a hob applied at present. The generation of a conjugated worm is based on application of a tilted head-cutter (grinding tool) as well. The bearing contact of the gear drive is localized and is oriented longitudinally. A predesigned parabolic function of transmission errors for reduction of noise and vibration is provided. The stress analysis of the gear drive is performed using a three-dimensional finite element analysis. The contacting model is automatically generated. The developed theory is illustrated with numerical examples.

1. Introduction

Invention of face worm gear drives with conical and cylindrical worms by O. Saari [13, 14] was a substantial contribution. One of the greatest advantages of such drives is the higher contact ratio as the result of simultaneous contact of several pairs of teeth during the cycle of meshing. Initially the design of the invented gear drives was based on application of worms provided by axial profiles as straight lines. The worms have been designed as helicoids of a constant lead angle. Investigation of the invented gear drives has been performed by Saari and his followers [13, 14], Goldfarb [3, 4], Dudas [1], and other researchers. Spiroid worm gear drives have been discussed as well in the Gear Handbook [16].

A new modification of the face gear drives has been proposed by Litvin, De Donno, Argentieri et al [8, 9, 10, 11]. The bearing contact of the proposed gear drives is a localized and a favorable shape of transmission errors for reduction of noise and vibration is provided. This is achieved by double crowning of the worm.

The generation of face worm gear drives of all types of existing design is based on application of a hob for generation of the face-gear. The hob is similar to the worm of the drive. The disadvantage of such method of generation is the low precision of a hob used as a generating tool especially in the case of small dimensions of hob.

The new geometry proposed in this paper is based on application of head-cutters or head grinding tools that have higher precision and larger dimensions in comparison with a hob and enable to provide a higher productivity of the process of generation. The gear drives of new geometry may be generated similar to the generation of spiral bevel gears and hypoid gears [7, 15]. The proposed new face worm gear drives (with conical and cylindrical worms) are provided with a localized bearing contact and predesigned parabolic function of transmission errors of low level. Such a function is able to absorb discontinuous linear functions of transmission errors caused by errors of alignment [8, 9]. Therefore vibrations and noise of gear drives might be reduced.

The localization of bearing contact is achieved by the mismatch of surfaces of generating head tools applied for generation of the face worm-gear and the worm. Figures 1 and 2 show in 3D space face worm gear drives with conical and cylindrical worms that have been investigated in this paper. The proposed new design of a face gear drive is based on adaptation of the design parameters of a similar gear drive of existing design (based on generation of face-gear by a hob). This permits a common analysis between both designs but affects the dimensions of applied head cutters (Section 2).

The contents of the paper cover the generation and analytical determination of tooth surfaces of the face-gear and the worm, simulation of meshing and contact, and stress analysis.

The theory developed is illustrated with numerical examples.

The determination of conjugation of tooth surfaces of the proposed gear drive required the application of theory of enveloping that is the subject of differential geometry and theory of gearing represented in the works by Zalgaller [17], Zalgaller and Litvin [18], Favard [2], Korn [6], Litvin [8, 9], and other works.

2. Basic Ideas for Generation of Face-Gear and Conical Worm

Face Worm-Gear Generation. The generation is performed by a tilted head-cutter with straight line profiles of blades (Fig. 3). The tilt of the head-cutter avoids interference of the head-cutter with teeth that neighbor to the space being generated.

Figure 4 illustrates schematically the generation of the face-gear. The tool is mounted on the cradle c of the generating machine (Fig. 4) and performs rotation about the tool axis. The face-gear Σ_2 and the cradle c are fixed and the tooth surface of the face-gear is generated as the copy of the tool surface.

Indexing of face-gear has to be provided for generation of each space of the gear.

Blades of the gear head-cutter are shown in Fig. 5(a). The angles α_g of blade profile are of different magnitude for the convex and concave sides of the space of the face worm-gear. Circular arc profiles of the blade fillet are provided for the generation of the fillet of the gear.

Worm generation. The generation of the worm is performed by a tilted head-cutter mounted on the cradle d of the generating machine (Fig. 6). The worm and the cradle d perform related rotations determined as

$$\frac{\omega^{(w)}}{\omega^{(d)}} = \frac{N_2}{N_1} \tag{1}$$

where N_2 and N_1 are the number of teeth of the face-gear and number of threads the worm, respectively. The rotation of the head-cutter is provided for obtaining the desired velocity of cutting (grinding) and is not related with the meshing of cradle d and the worm. Figure 7 illustrates the installment of the worm with respect to the cradle d.

The process of generation of the worm simulates its meshing with the face-gear. The face-gear is represented in Fig. 7 as cradle d that carries the head-cutter. The worm head-cutter and cradle d may be considered as rigidly connected to each other in the process of meshing of cradle d with the worm. The surface of the head-cutter simulates the tooth surface of the face worm-gear.

The process of worm generation provides for the gear drive: *(i)* localization of bearing contact, and *(ii)* a parabolic function of transmission error. Localization of contact is achieved by deviation of profiles of blades of worm head-cutter with respect to the blades of gear head-cutter (see Section 3). Parabolic function of transmission errors is provided by variation of distance $E_m(\psi_1)$ (Fig. 7) during the worm generation where (ψ_1) is the angle of worm rotation performed during the process of worm generation.

3. Analytical Determination of Face-Gear Tooth Surface Conjugated to Conical Worm

The derivation of face-gear tooth surface of new design is based on the following procedure:

(i) Derivation of face gear tooth surfaces Σ_2^* of existing design generated by a hob.

(ii) Determination of pitch point P of existing design.

(iii) Determination of circle C of surface Σ_2^* that passes through point P and two other points of Σ_2^*. The radius of circle C is the radius of the head-cutter to be used for generation of face-gear tooth surface of new design.

(iv) Determination of profile of blade of head-cutter considering the cross-section of Σ_2^* at pitch point P.

(v) Derivation of surface of head-cutter applied for generation of surface Σ_2^* of new design.

(vi) Determination of installment of the head-cutter on the cradle c (Fig. 4).

(vii) Determination of surface Σ_2 of the new design as the copy of the gear head-cutter surface.

The described procedure is applied for derivation of both tooth sides.

Derivation of Face-Gear Tooth Surface Σ_2^* of Existing Design. Surface Σ_2^* is determined in coordinate system S_2 rigidly connected to the face-gear as follows [10]:

$$\mathbf{r}_2^* = \mathbf{r}_2^*(u_h, \theta_h, \psi_h) \tag{2}$$

$$\left(\frac{\partial \mathbf{r}_2^*}{\partial u_h} \times \frac{\partial \mathbf{r}_2^*}{\partial \theta_h}\right) \cdot \frac{\partial \mathbf{r}_2^*}{\partial \psi_h} = f^*(u_h, \theta_h, \psi_h) = 0 \tag{3}$$

Here: equations (2) represent the family of hob surfaces in S_2; equation (3) is the equation of meshing; (u_h, θ_h) are the parameters of hob surface; ψ_h is the generalized parameter of motion in the process of generation of surface Σ_2^* of existing design.

Equations (2) and (3) represent surface Σ_2^* by three related parameters.

We may represent Σ_2^* in two parameter form by using the theorem of implicit function system existence as follows [6, 8, 9, 17, 18]:

(i) Consider that point $M(u_h^0, \theta_h^0, \psi_h^0)$ satisfies equation $f_h^* = 0$ and an inequality

$$\left|\frac{\partial f^*}{\partial u_h}\right| + \left|\frac{\partial f^*}{\partial \theta_h}\right| \neq 0 \tag{4}$$

is observed at M, say because $\partial f^{*}/\partial\theta_h \neq 0$. Therefore equation $f_h^{*}=0$ may be solved in the neighborhood of M by function

$$\theta_h = \theta_h(u_h,\psi_h), \qquad \theta_h \in C^1 \tag{5}$$

Then surface Σ_2^{*} may be represented locally as

$$\mathbf{r}_2^{*}(u_h,\theta_h(u_h,\psi_h),\psi_h)=\mathbf{R}_2^{*}(u_h,\psi_h) \tag{6}$$

Determination of Pitch Point *P*. Pitch point P is the point of tangency of the cone of the worm and the pitch cone of the existing design (Fig. 8). Determination of P requires application of equations (2) and (3) and parameters E_m and L of installment of the worm.

Design Parameters and Installment of Generating Tool. The generating tool is installed in a plane (designated by Π) that is determined by three chosen points of surface Σ_2^{*} generated by a hob. These points are designated as A_1, P, and A_2 (Fig. 8(a)) where P is the pitch point, A_1 and A_2 are the points of Σ_2^{*} that are generated by the middle point of the axial profile of the hob.

Plane Π is shown in 3D (Fig. 8(b)). Circle C that lies in Π and passes through A_1, P, and A_2 is of radius ρ determined by using the coordinates of A_1, P, and A_2. The axis z_g of the generating tool is perpendicular to plane Π and passes through point O_g that is the center of circle C. The orientation of plane Π is determined with respect to plane T of the drawings (Fig 8(b)). The installment of the generating tool with respect to coordinate system S_2 rigidly connected to face worm-gear is determined by direction cosines of coordinate system S_g of the generating tool and position vector $\overline{0_2 0_g}$.

The blade of the gear head-cutter is a straight line (Fig. 5(a)) and profile angle α_g is determined from the condition that the straight line is a tangent to the cross-section of the face-gear at point P.

Derivation of Surface of Gear Head Cutter. The surface of the head-cutter is illustrated in Fig. 5(a). It may be represented as a combination of a cone in the working part and a torus of the fillet part. The gear tooth surface is generated as a copy of the tool surfaces and is represented in S_2 by the matrix equation

$$\mathbf{r}_2(u_g,\theta_g)=\mathbf{M}_{2g}\mathbf{r}_g(u_g,\theta_g) \tag{7}$$

Here: (u_g,θ_g) are the surface coordinates of the head-cutter represented by vector function $\mathbf{r}_g(u_g,\theta_g)$. Matrix $\mathbf{M}_{2g}$ describes the coordinate transformation from the tilted head-cutter to coordinate system S_2. Elements of matrix $\mathbf{M}_{2g}$ are determined by position vector $\overline{0_2 0_g}$ and direction cosines of coordinate axes of S_g (Fig. 8).

Avoidance of Interference. The investigation of avoidance of interference may be accomplished analytically but it requires derivation of equations of tooth surfaces of many teeth and equations of their

intersection with the head-cutter. The authors have used computer graphics as shown in Fig. 9. Avoidance of interference may require in some case the increase of the tilt of the head-cutter.

4. Analytical Determination of Thread Surface of the Worm

Coordinate systems applied for derivation are shown in Fig. 10. Fixed coordinate systems S_n and S_m are rigidly connected to the frame of the generating machine. Movable coordinate systems S_d and S_1 are rigidly connected to the cradle d of the generating machine and the worm, respectively. Schematics of worm generation are shown in Figs. 6 and 7.

The worm is generated by a tilted head-cutter (Figs. 6 and 7).

The blades of the head-cutter are of parabolic profile and deviate from the straight line profiles of the gear head-cutter (Fig. 11). Such mismatch is necessary for the localization of bearing contact of the gear drive.

The installment of the worm during the generation is shown in Figs. 7 and 10. We emphasize that the shortest distance E_m between the worm and the cradle is executed in the cycle of meshing as a parabolic function

$$E_m(\psi_1) = E_0 + a_{pl}\psi_1^2 \tag{8}$$

where E_0 is the normal value of the center distance; a_{pl} is the parabola coefficient of the plunge $a_{pl}\psi_1^2$.

The plunge ($a_{pl}\psi_1^2$) provides a predesigned parabolic function of transmission errors of the gear drive (see Section 5).

Remembering that the worm is generated by the head-cutter that is installed on the cradle d (Fig. 6) whereas the worm and the cradle d perform related rotations. The worm thread surface is determined as the envelope to the family of head-cutter surfaces as follows:

$$\mathbf{r}_1(u_w,\theta_w,\psi_1) = \mathbf{M}_{1d}\mathbf{M}_{dw}\mathbf{r}_w(u_w,\theta_w) \tag{9}$$

$$\left(\frac{\partial \mathbf{r}_1}{\partial u_w}\times\frac{\partial \mathbf{r}_1}{\partial \theta_w}\right)\cdot\frac{\partial \mathbf{r}_1}{\partial \psi_1} = f(u_w,\theta_w,\psi_1) = 0 \tag{10}$$

Here: $\mathbf{r}_w(u_w,\theta_w)$ is the vector function that determines the surface of the head-cutter in coordinate system S_d of the cradle d : (u_w,θ_w) are the surface parameters of the generating tool (the head-cutter or the grinder); ψ_1 is the generalized parameter of motions; $\mathbf{M}_{1d}$ and $\mathbf{M}_{dw}$ describe the coordinate transformation from S_d to S_1 and S_w to S_d.

Matrix equation (9) determines the family of head-cutter surfaces in S_1. The cradle d and the head-cutter are considered in derivations as one rigid body. Rotations of the head-cutter and cradle d are considered in derivations as rotation of one rigid body. Rotation of the head-cutter about its axis provides the desired velocity of cutting and does not affect the process of generation.

Equation (10) is the equation of meshing. The cross product in equation of meshing is the normal to the surface of the head-cutter represented in S_1. Vector $\partial \mathbf{r}_1 / \partial \psi_1$ is equivalent to the vector of relative velocity in meshing of the head-cutter and the worm. Figure 12 represents in 3D space the worm thread surface Σ_1.

The generated surface Σ_1 requires separate generation of both sides of thread surfaces because the plunging motion (see equation (8)) may require different parabola coefficients for each side. Multithread worm requires separate generation of each surface of the thread.

5. Simulation of Meshing and Contact

The purpose of simulation of meshing and contact is for determining the bearing contact and transmission errors of a misaligned face worm gear drive. The computerized procedure for simulation of meshing and contact is performed by application of computer programs that were developed.

The meshing of misaligned gear tooth surfaces is based on continuous tangency of contacting tooth surfaces (Fig. 13).

Surfaces Σ_1 and Σ_2 of the worm and face worm gear and their normals are represented in a fixed coordinate system S_f. The continuous tangency of Σ_1 and Σ_2 is represented by equations:

$$\mathbf{r}_f^{(1)}(u_1, \theta_1, \phi_1) - \mathbf{r}_f^{(2)}(u_2, \theta_2, \phi_2) = \mathbf{0} \tag{11}$$

$$\mathbf{n}_f^{(1)}(u_1, \theta_1, \phi_1) - \mathbf{n}_f^{(2)}(u_2, \theta_2, \phi_2) = \mathbf{0} \tag{12}$$

For the purpose of simplicity the designations of variables of equations (11) and (12) in comparison with previous designations were changed. The solution of equations (11) and (12) is an iterative process and permits the determination of the paths of contact on tooth surfaces of the face-gear and the worm and transmission errors [8, 9]. Figure 14(a) (the output of TCA (Tooth Contact Analysis)) shows that the function of transmission errors is obtained indeed as a parabolic function of low magnitude; Figs. 14(b) and 14(c) show that the bearing contact is localized indeed and it has a longitudinal direction.

The bearing contact is formed as a set of instantaneous contact ellipses (Figs. 14(b) and 14(c)). The orientation and magnitude of axes of contact ellipses are determined by the principal curvatures and directions of the contact tooth surfaces and their elastic approach [8, 9]. The output of TCA (Fig. 14) has been obtained for a gear drive with design parameters represented in Table 1 (see Section 6).

6. Stress Analysis

Preliminary Information. The goals of finite element analysis developed are the following:

(i) Investigation of formation of the bearing contact during the cycle of meshing.
(ii) Determination of the contact and bending stresses.
(iii) Determination of the contact ratio.

A stress analysis has been performed by application of finite element analysis [19] by a general purpose computer program [5].

The finite element method requires definition of the contacting surfaces and establishment of the boundary conditions.

The approach developed by the authors has the following advantages:

(a) Using the equations of the tooth surfaces and of the fillets and considering the portion of the rim, the finite element models are generated automatically. Loss of accuracy introduced by CAD computer programs for the generation of the mesh is avoided.

(b) The proposed approach does not require an assumption on the load distribution in the contact area. To get the contact area and the stresses the contact algorithm of the general purpose computer program [5] is used.

(c) Finite element models are developed numerically at the chosen point of the path of contact and at the chosen installment of the gear. Stress convergence is assured because the face-gear and the worm are in contact at least in one point.

(d) Finite element models of five pairs of teeth are applied and therefore the boundary conditions are far enough from the loaded areas of the teeth.

Development of Finite Element Models. The development of finite element analysis using CAD computer programs in an interactive way is time expensive, requires skilled users for application of computer programs and has to be done for every case of development of gear geometry, position of meshing and installment desired. The approach developed is free of all these disadvantages and is summarized as follows:

Step 1: It is possible to represent analytically the volume of the tooth using the equations of the surfaces and the portions of the corresponding rim. Fig. 15(a) shows the designed body for one tooth model of the face-gear.

Step 2: Six surfaces (Fig. 15(b)) determined analytically divide the volume in six parts and control the discretization of these tooth subvolumes into finite elements.

Step 3: Analytical determination of node coordinates is performed automatically by choosing the desired number of elements in longitudinal and profile directions (Fig. 15(c)). All the nodes of the finite element analysis are determined analytically and the points of the intermediate surfaces of the tooth belong to the real gear tooth surfaces.

Step 4: Discretization of the model by finite elements (using the nodes determined previously) is accomplished as shown in Fig. 15(d).

Step 5: The boundary conditions for the face-gear and the worm are set automatically under the following conditions:

(i) Nodes on the bottom of the worm rim are considered as fixed (Fig. 16(a)).

(ii) Nodes on the two sides and the bottom part of the face-gear rim form a rigid surface (Fig. 16(b)). Such rigid surface is a three-dimensional structure that may perform translation and rotation but cannot be deformed.

(iii) Considering the face-gear rim rigid surfaces the variables of motions of the face-gear (its translation and rotation) are associated with a single point M located on the axis of the face-gear chosen as the reference point. Point M has only one degree-of-freedom (rotation about the face-gear axis) and all the other degrees of freedom are fixed. The torque T is applied directly to the face-gear at its reference point M.

Step 6: The definition of the contact surfaces necessary for the finite element analysis is accomplished automatically, identifying all the elements of the model required for the formation of such surfaces.

A symmetric master-slave method has been applied. This method causes the algorithm to treat each surface as a master surface.

Numerical Example: The finite element analysis has been performed for a face-worm gear drive with conical worm of common design parameters represented in Table 1. For the analysis the model of the whole worm (Fig. 17) and the whole face-gear (Fig. 18) have been substituted by a model of five-pair of teeth in meshing (Fig. 19) in order to save computational time. Elements C3D8I of first order have been used for the finite element mesh. The total number of elements is 55672 with 68671 nodes. The material used is steel with Young's Modulus E=2.068 x 10^8 mN/mm and Poisson's ratio 0.29. The torque applied to the face-gear is 50 N·m. Figures 20, 21, and 22 show how the bearing contact looks at the beginning, at the middle, and at the end of a cycle of meshing.

Table 1: Design Parameters of Face Worm Gear Drive with Conical Worm

Number of threads of the worm	2
Number of teeth of the face-gear	60
Gear ratio	30
Axial module	1.334 mm
Convex side pressure angle	10.0 deg
Concave side pressure angle	30.0 deg
Shaft angle γ_m	90.0 deg
Minimal distance between the axes E_m	35.0 mm
Worm axial displacement L	29.907 mm
Worm pitch diameter D_p	11.480 mm
Worm cone angle	5.0 deg
Inner radius of the face-gear	38.53 mm
Outer radius of the face-gear	52.50 mm
Mean radius of the head-cutter	24.398 mm
Plunging coefficient a_{pl} (convex side)	0.003 mm
Plunging coefficient a_{pl} (concave side)	-0.003 mm

The results obtained by finite element analysis confirm the longitudinal path of contact and the avoidance of edge contact. Figure 23 shows the variation of bending and contact stresses on the face-gear from the beginning of the contact to the end of contact on one tooth of the face-gear.

The stresses are represented as unitless parameters in function of the worm rotation

$$\sigma_{m1} = \frac{\sigma_1}{\sigma_{\max 1}} \tag{13}$$

$$\sigma_{m2} = \frac{\sigma_2}{\sigma_{\max 2}} \tag{14}$$

where σ_1 and σ_2 are the bending and contact stresses of Von Mises and $\sigma_{\max 1}$ and $\sigma_{\max 2}$ are the maximum bending and contact stresses of Von Mises on the face-gear. In the example developed, $\sigma_{\max 1} = 168\ \mathrm{N/mm^2}$ and $\sigma_{\max 2} = 1090\ \mathrm{N/mm^2}$. The load is always shared by 3 pairs of teeth, therefore the contact ratio is 3.

7. Geometry, TCA, and Stress Analysis of Face Worm Gear Drive with Cylindrical Worm

The geometry discussed is considered as a particular case of the geometry of the gear drive with a conical worm. The generation of the face-gear and the worm are based on the same principles as described is sections 2, 3, and 4. It requires tilted head-cutters as well but generally of a larger value of the tilt of the tool. Figure 24 shows the cylindrical worm that is generated by a tilted head-cutter.

The TCA has been performed for a gear drive of design parameters represented in Table 2.

Table 2: Design Parameters of Face Worm Gear Drive with Cylindrical Worm

Number of threads of the worm	2
Number of teeth of the face-gear	60
Gear ratio	30
Axial module	1.334 mm
Convex side pressure angle	10.0 deg
Concave side pressure angle	30.0 deg
Shaft angle γ_m	90.0 deg
Minimal distance between the axes E_m	35.0 mm
Worm axial displacement L	29.907 mm
Worm pitch diameter D_p	11.480 mm
Worm cone angle	0.0 deg
Inner radius of the face-gear	39.763 mm
Outer radius of the face-gear	49.753 mm
Mean radius of the head-cutter	23.105 mm
Plunging coefficient a_{pl} (convex side)	0.003 mm
Plunging coefficient a_{pl} (concave side)	-0.003 mm

A predesigned parabolic function of transmission errors indeed absorbs the discontinuous functions of transmission errors caused by errors of alignments (Fig. 25(a)). Figures 25(b) and 25(c) show that the bearing contact of a misaligned gear drive is localized and directed longitudinally as designed. The bearing contact is localized, and the path of contact is directed longitudinally.

Stress analysis has been developed following the principles exposed in Section 6. A numerical example has been accomplished for a gear drive of design parameters represented in Table 2. Figure 26 shows the finite element model of five pairs of teeth. The torque applied to the face-gear is 50 N·m. The total number of elements is 55672 with 68671 nodes. Variation of bending and contact stresses on the face-gear are shown in Fig. 27. The maximum bending stress (σ_{max1}) is 195 N/mm^2. The maximum contact stress (σ_{max2}) is 960 N/mm^2. The load is shared by three pairs of teeth during all the cycle of meshing, therefore the contact ratio is 3.

8. Conclusions

Based on the performed research, the following conclusions might be drawn.

1. A new geometry of face worm gear drives with conical and cylindrical worms is proposed. The geometry is based on generation of face worm-gear by a tilted head-cutter or a grinding tool instead of a hob. The conjugated thread surface of the worm is generated by a head-cutter or a grinding tool as well.
2. The tooth surface of the face worm-gear and the worm thread surface are determined analytically.
3. The bearing contact of the face worm gear drive is localized due to the mismatch of generating surfaces. The obtained bearing contact is oriented longitudinally.
4. A predesigned parabolic function of transmission errors of a low magnitude is provided that reduces the noise and vibration of the gear drive.
5. Variation of the surface is obtained by tool plunging during the worm generation.
6. An enhanced approach for stress analysis has been developed that automates the development of the finite element contacting model.

References

[1] Dudas, I., The Theory and Practice of Worm Gear Drives, Penton Press, 2000.

[2] Favard, J., Course of Local Differential Geometry, Gauthier-Villars, Paris (in French, translated into Russian), 1957.

[3] Goldfarb, V.I., Airapetov, E.L.e.S., Novosyelov, V.Yu., Analytical and Experimental Assessment of Spiroid Gear Tooth Deflection, Proceedings of the 10th World Congress on TMM, vol. 6, Oulu, Finland, June 20–24, 1999, p. 2257–2262.

[4] Goldfarb, V.I., Kuniver A.S., Koshin D.V., Investigation of spiroid gear tooth tangency under action of errors, Proceedings of the International Conference on Gearing, Transmission and Mechanical Systems, Notthingam, London, 2000, p. 65–73.

[5] Hibbit, Karlsson & Sirensen, Inc., ABAQUS/Standard 6.1 User's Manual,1800 Main Street, Pantucket, RI 20860–4847, 1998.

[6] Korn, G.A. and Korn, T.M., Mathematics Handbook for Scientist and Engineers, McGraw-Hill, Inc., 2nd Ed., 1968.

[7] Krenzer, T.J., Computer Aided inspection of Bevel and Hypoid Gears, S.A.E. paper 831266, Milwaukee, WS, 1983.

[8] Litvin, F.L., Gear Geometry and Applied Theory, Prentice Hall, Inc., Englewood Cliffs, New Jersey, 1994.

[9] Litvin, F.L., Development of Gear Technology and Theory of Gearing, NASA Reference Publication 1406, ARL-TR-1500, 1998.

[10] Litvin, F.L. and De Donno M., Computerized design and generation of modified spiroid worm-gear drive with low transmission errors and stabilized bearing contact, Comput. Methods Appl. Mech. Engrg. 162(1998) 187–201.

[11] Litvin, F.L., Argentieri G. , De Donno M., Hawkins M., Computerized design, generation and simulation of meshing and contact of face worm-gear drives, Comput. Methods Appl. Mech. Engrg. 189(2000) 785–801.

[12] Nelson, W.N., Spiroid Gearing, Machine Design February 16, March 2–16, 1961.

[13] Saari, O.E., Speed-Reduction Gearing, Patent No. 2,696,125, United States Patent Office, 1954.

[14] Saari, O.E., Skew Axis Gearing, Patent No. 2,954,704, United States Patent Office, 1960.

[15] Stadtfeld, H.J., Handbook of Bevel and Hypoid Gears: Calculation, Manufacturing, and Optimization, Rochester Institute of Technology, Rochester, New York, 1993.

[16] Townsend, D.P. Dudley's Gear Handbook, McGraw-Hill, Inc., New York, 2nd Ed., 1991

[17] Zalgaller, V.A., Theory of Envelopes, Publishing House Nauka (in Russian), 1975.

[18] Zalgaller, V.A. and Litvin, F.L., Sufficient Condition of Existence of Envelope to Contact Lines and Edge of Regression on the Surface of the Envelope to the Parametric Family of Surfaces represented in Parametric Form, Proceedings of Universities: Mathematics (in Russian), Vol. 178, No. 3, pp. 20–23, 1977.

[19] Zienkiewicz, O.C. and Taylor, R.L., The Finite Element Method, John Wiley Sons, 5th Ed., 2000.

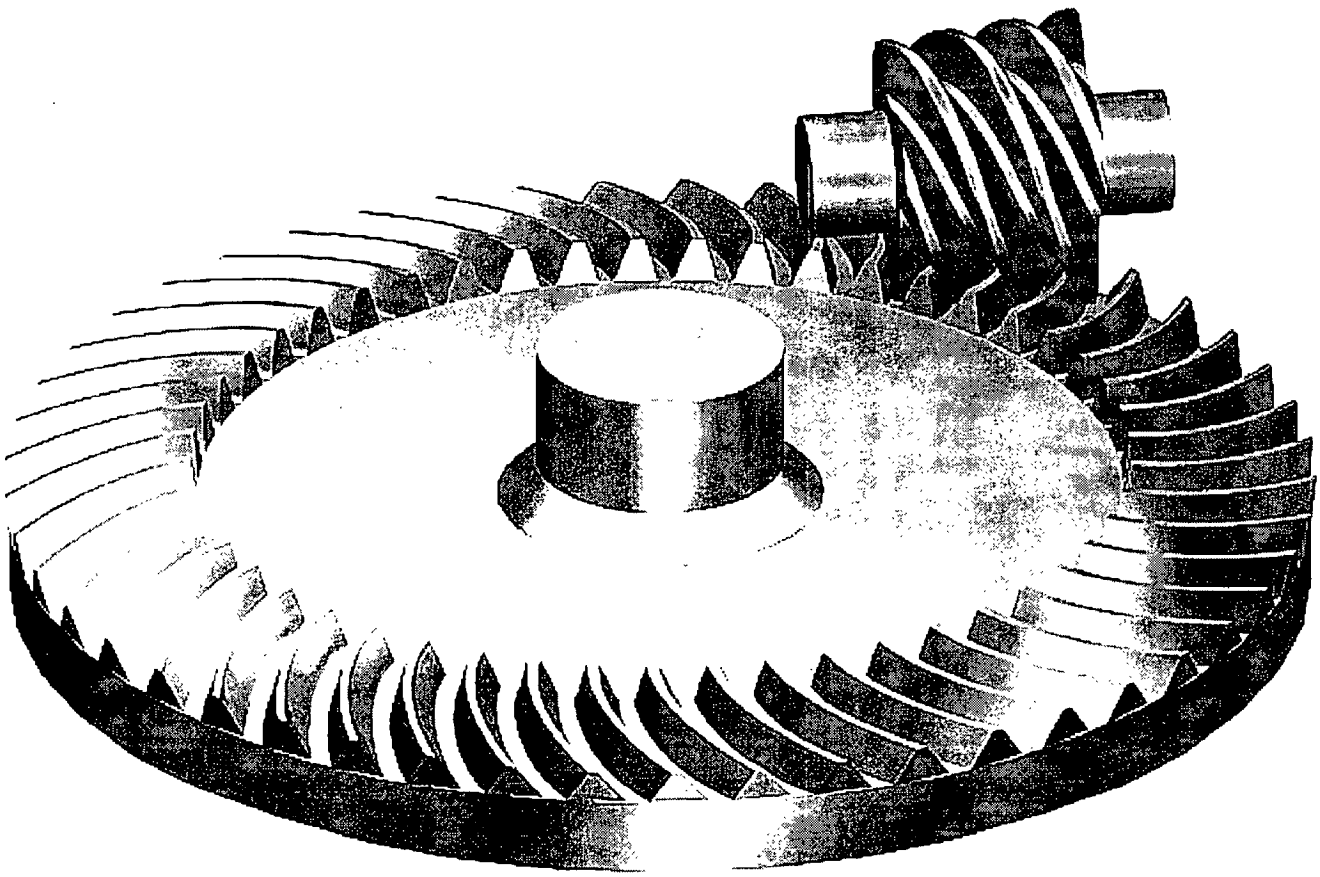

Figure 1: Face-worm gear drive with a conical worm

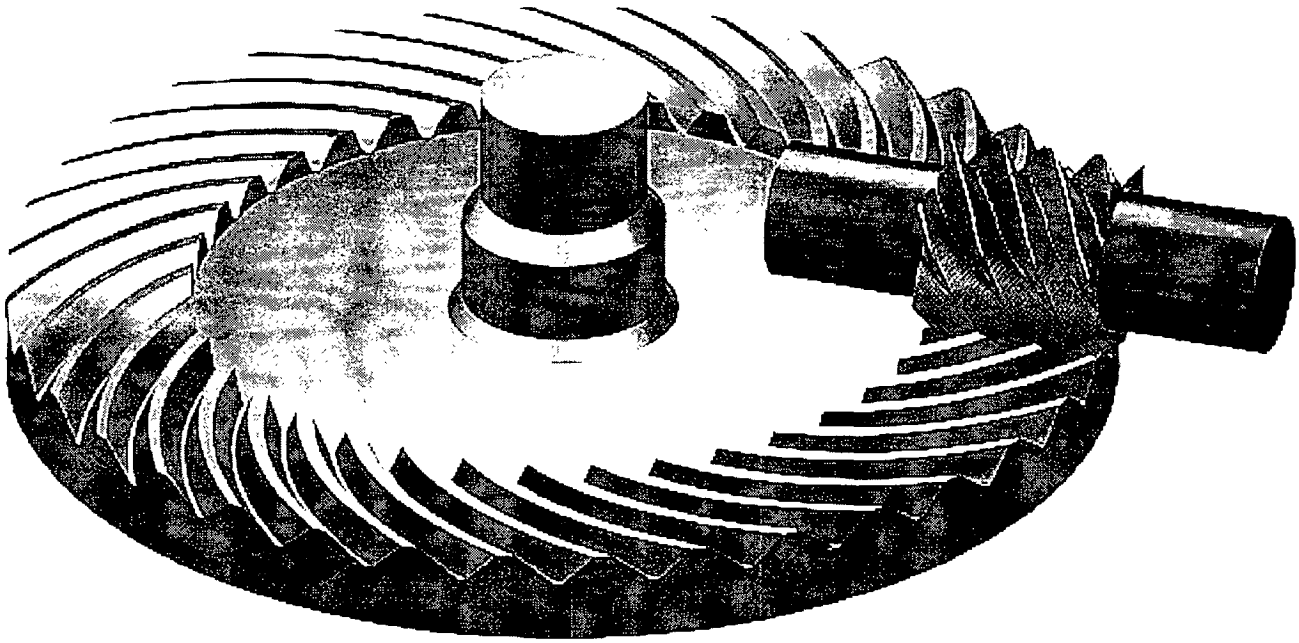

Figure 2: Face-worm gear drive with a cylindrical worm.

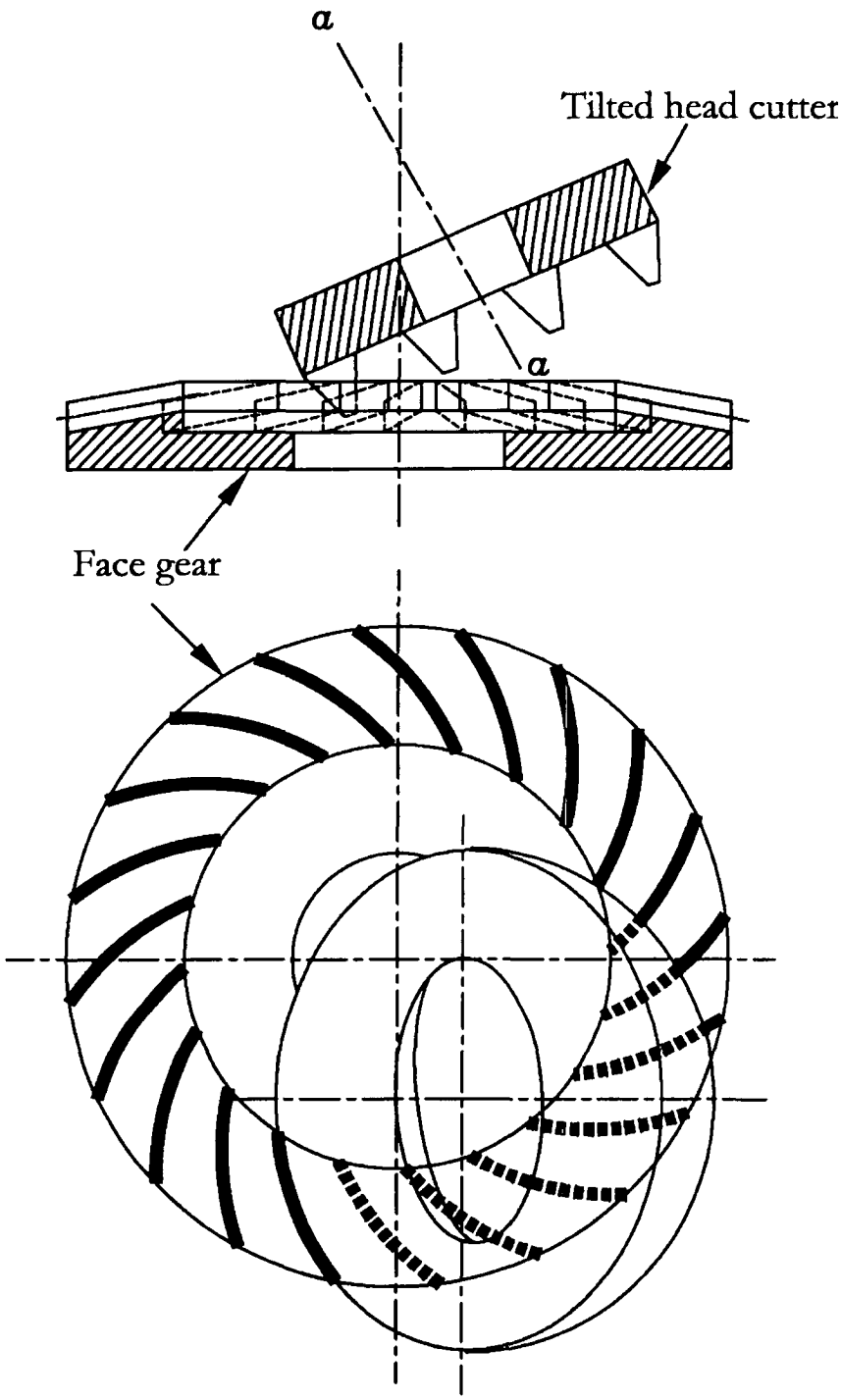

Figure 3: Generation of face worm-gear.

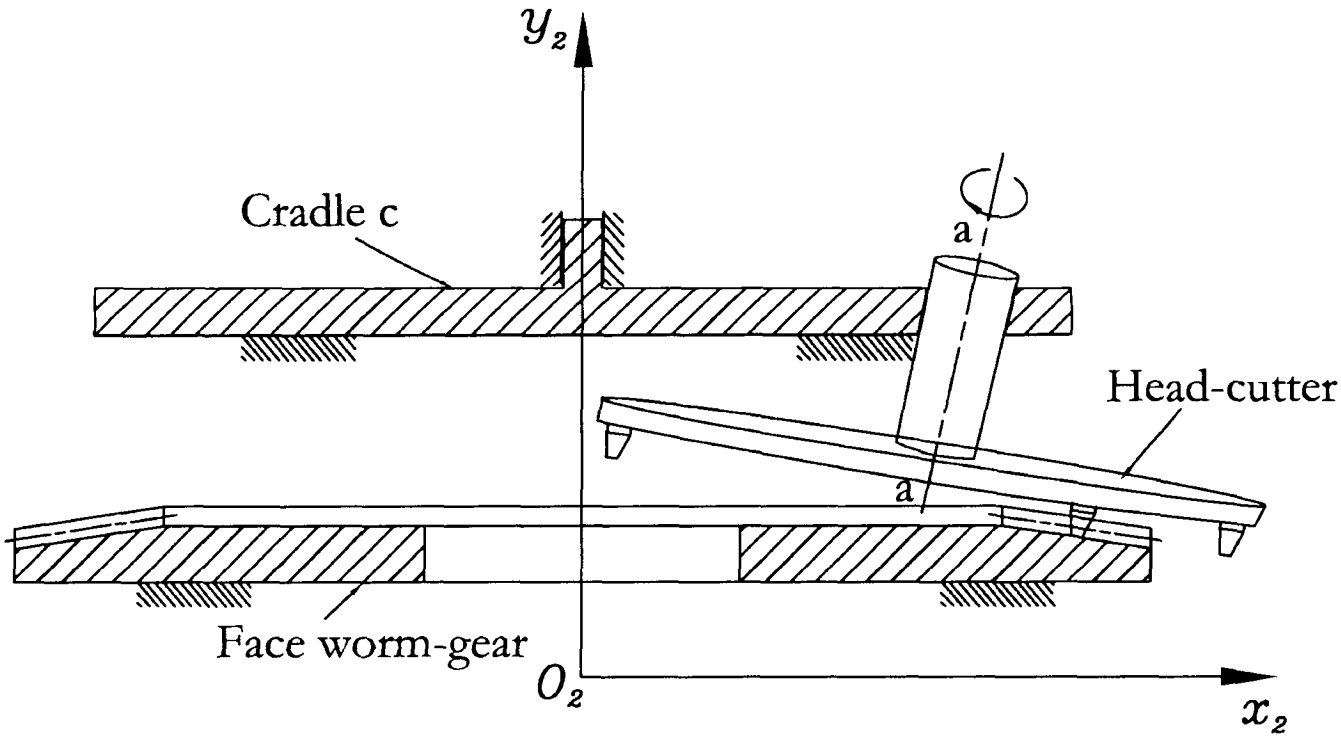

Figure 4: Schematic illustration of the head-cutter, the cradle c, and the face worm-gear.

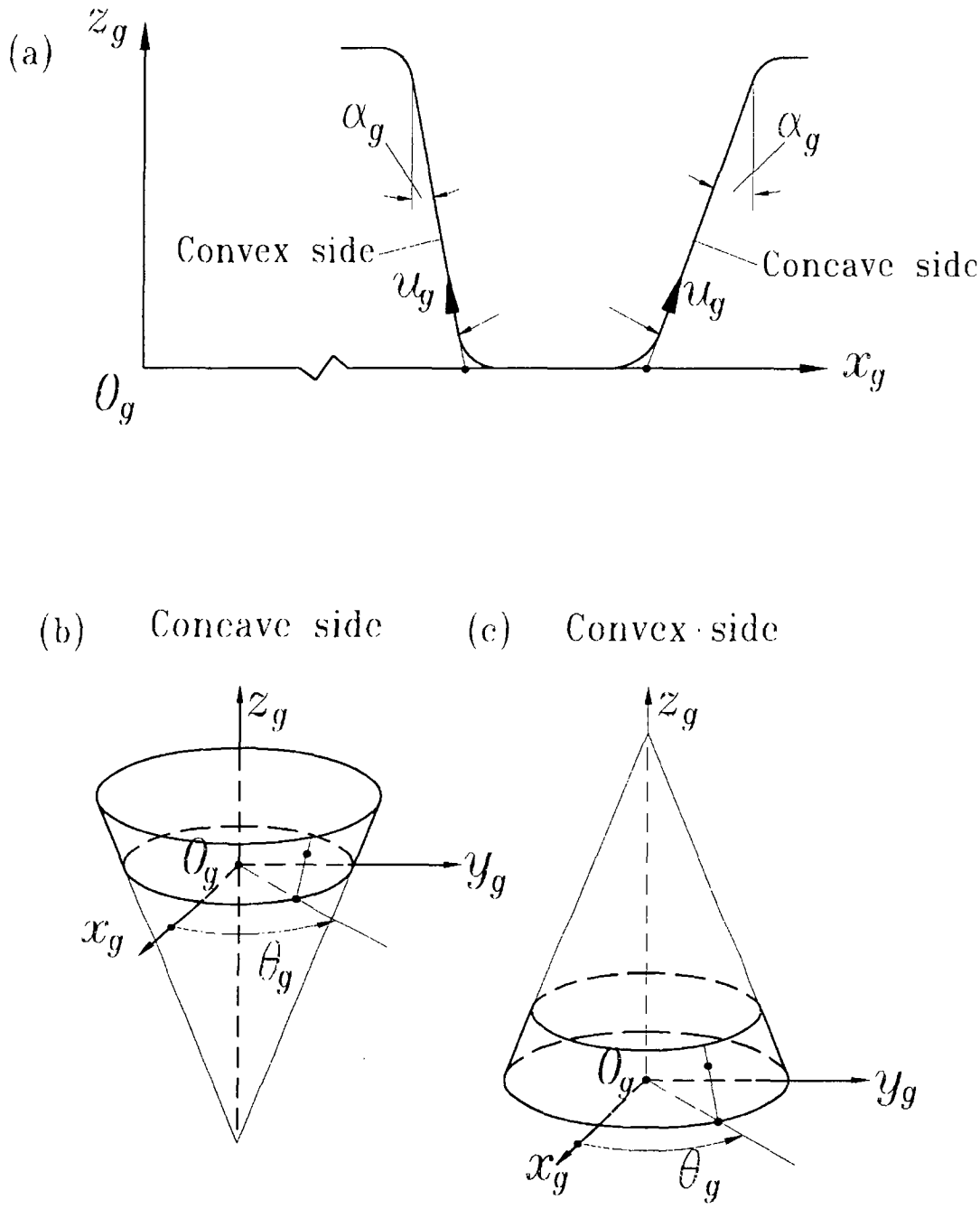

Figure 5: Blade and generating cones applied for generation of face worm-gear: (a) blade; (b) and (c) generating cones for concave and convex sides.

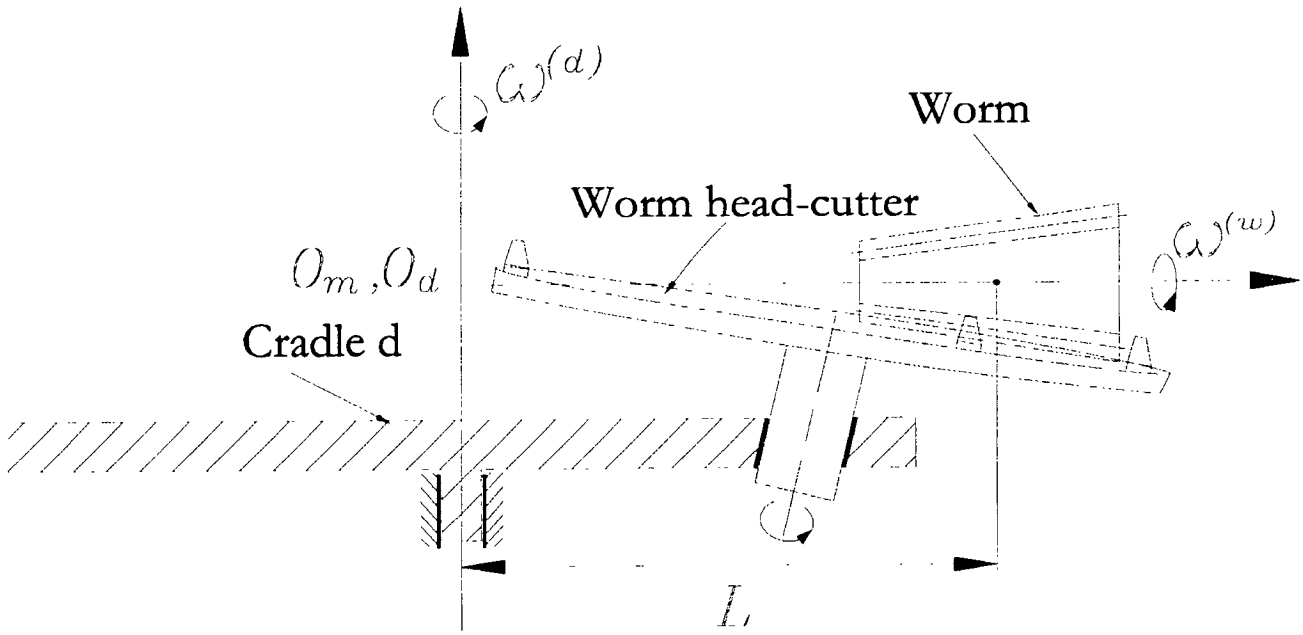

Figure 6: Schematic of worm generation.

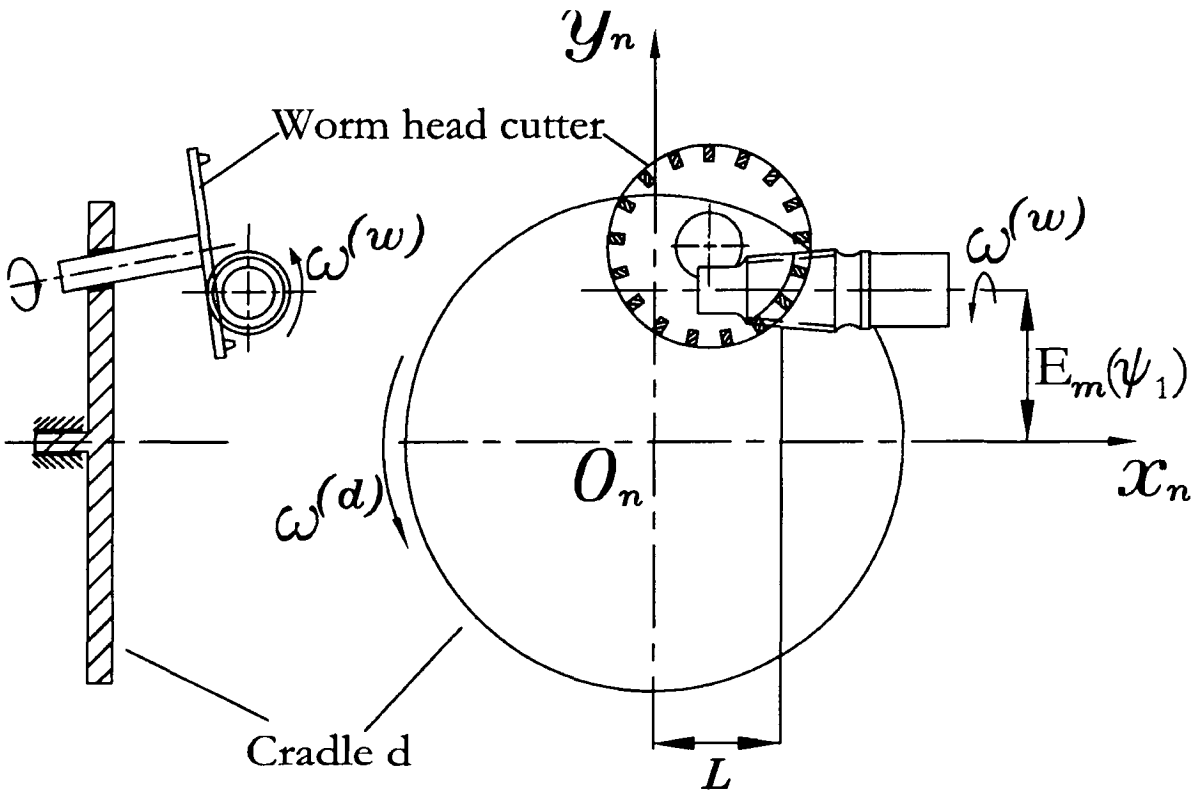

Figure 7: Installment of the worm with respect to the cradle *d*.

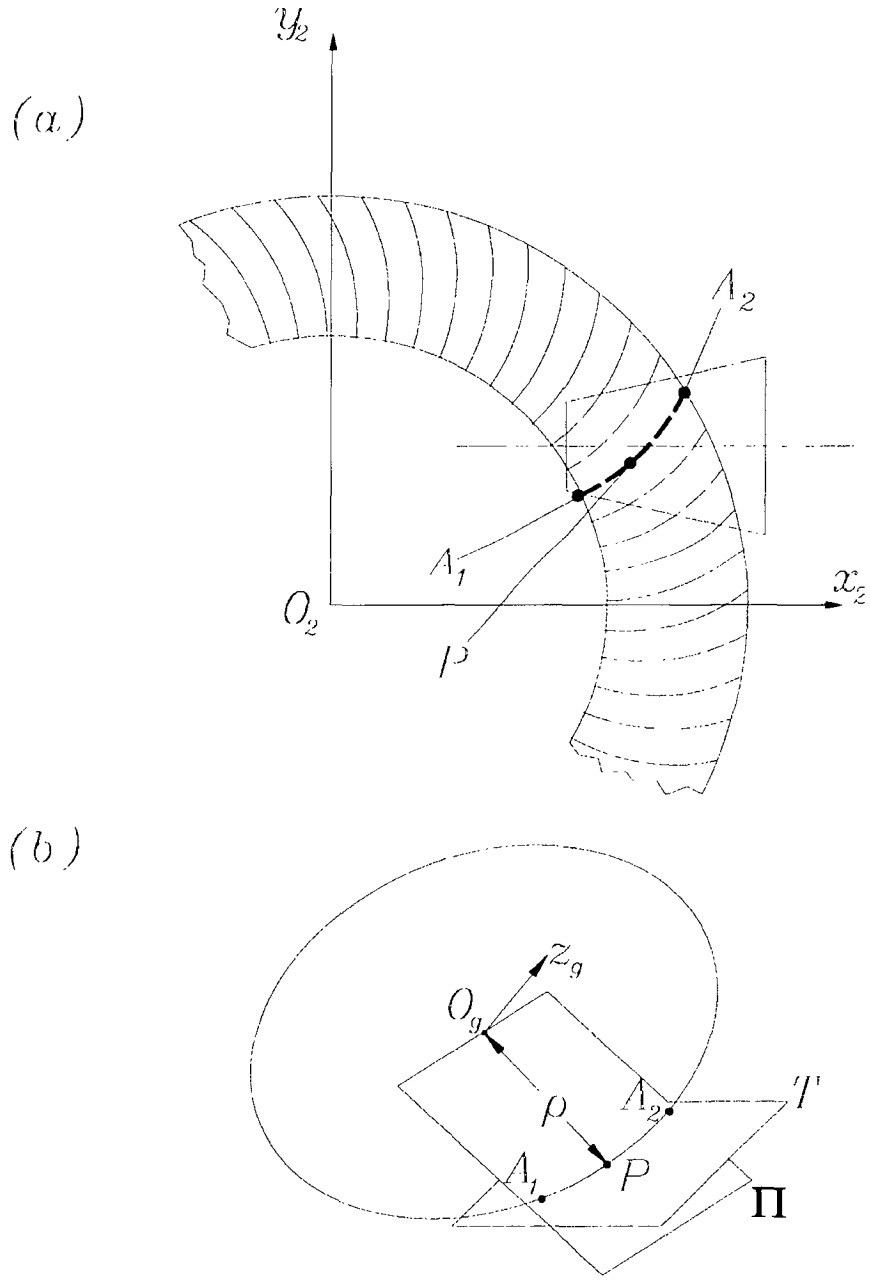

Figure 8: (a) Points A_1, P, and A_2 that belong to surface Σ_2^* generated by the hob; (b) Plane Π in 3D space, determined by the condition that Π passes through A_1, P, and A_2.

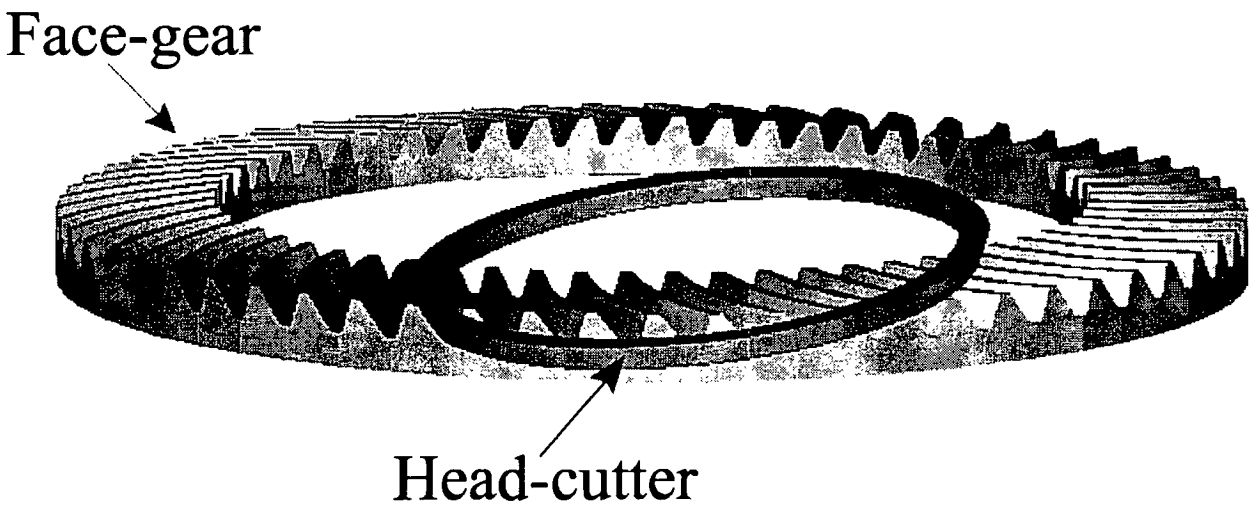

Figure 9: Face-gear and head-cutter in 3D space: avoidance of interference.

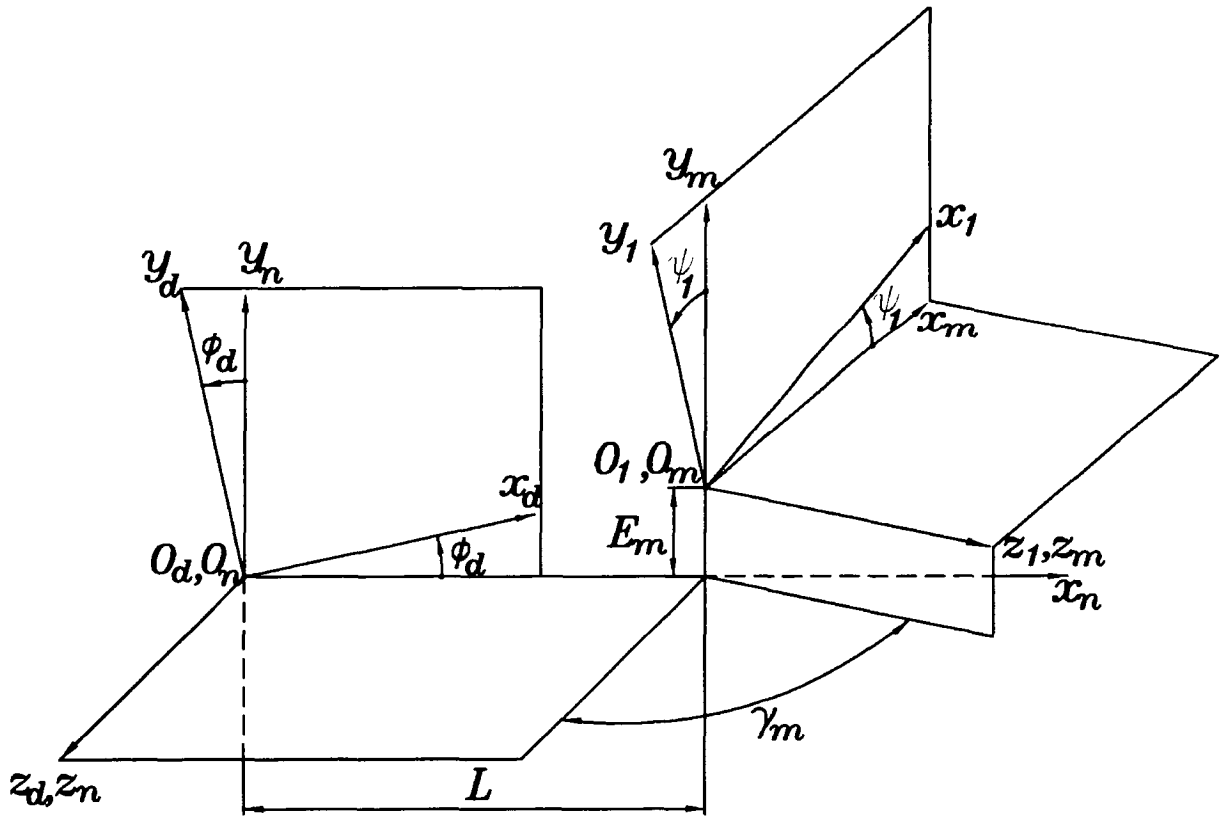

Figure 10: Coordinate systems applied for worm generation.

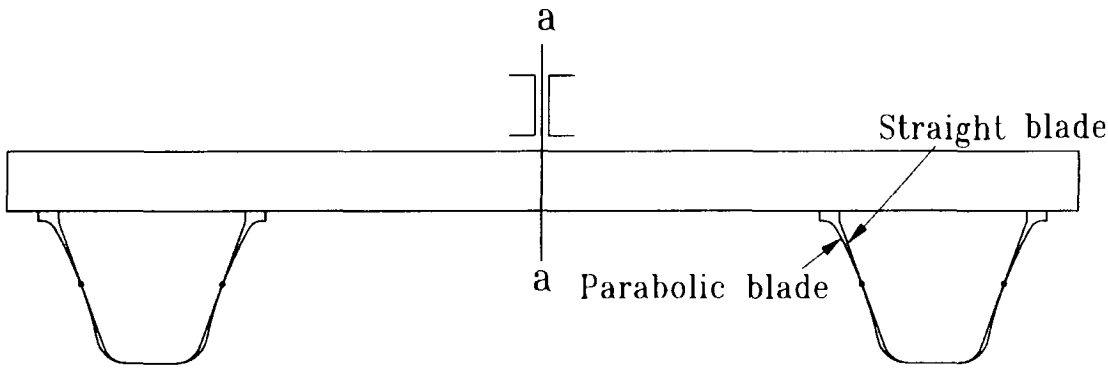

Figure 11: Illustration of mismatch of worm head-cutter surface.

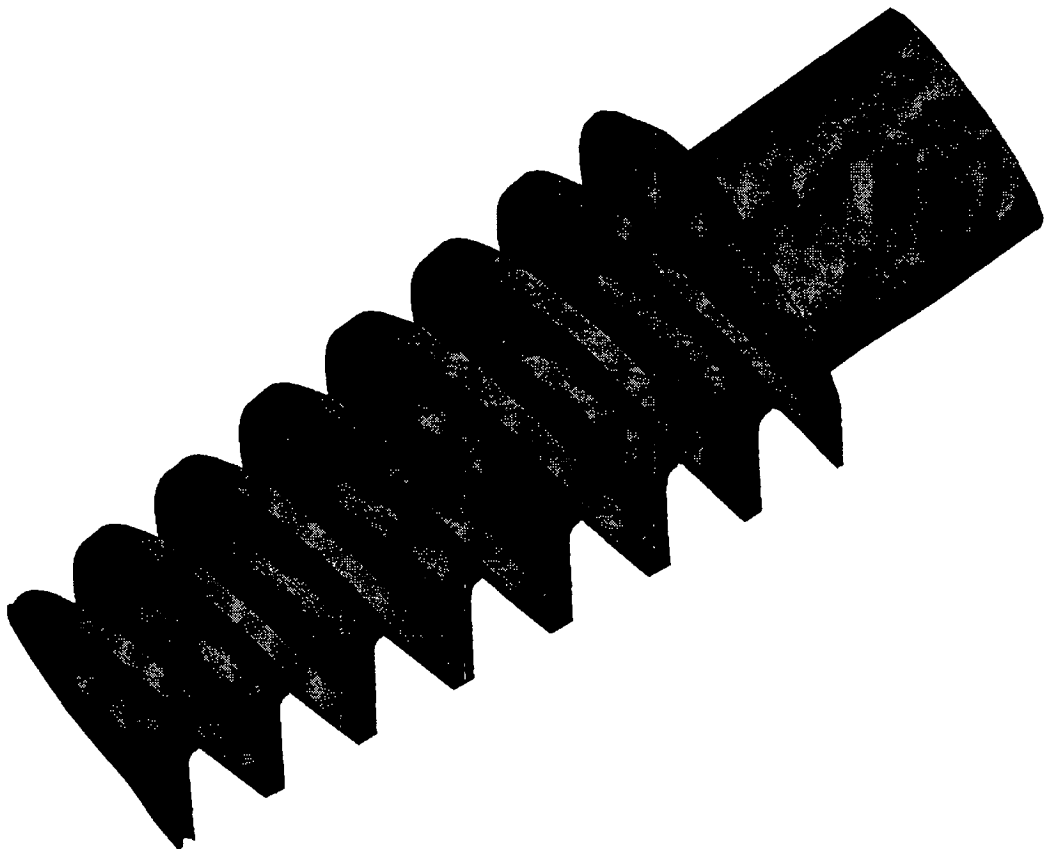

Figure 12: Conical worm thread surfaces in 3D space.

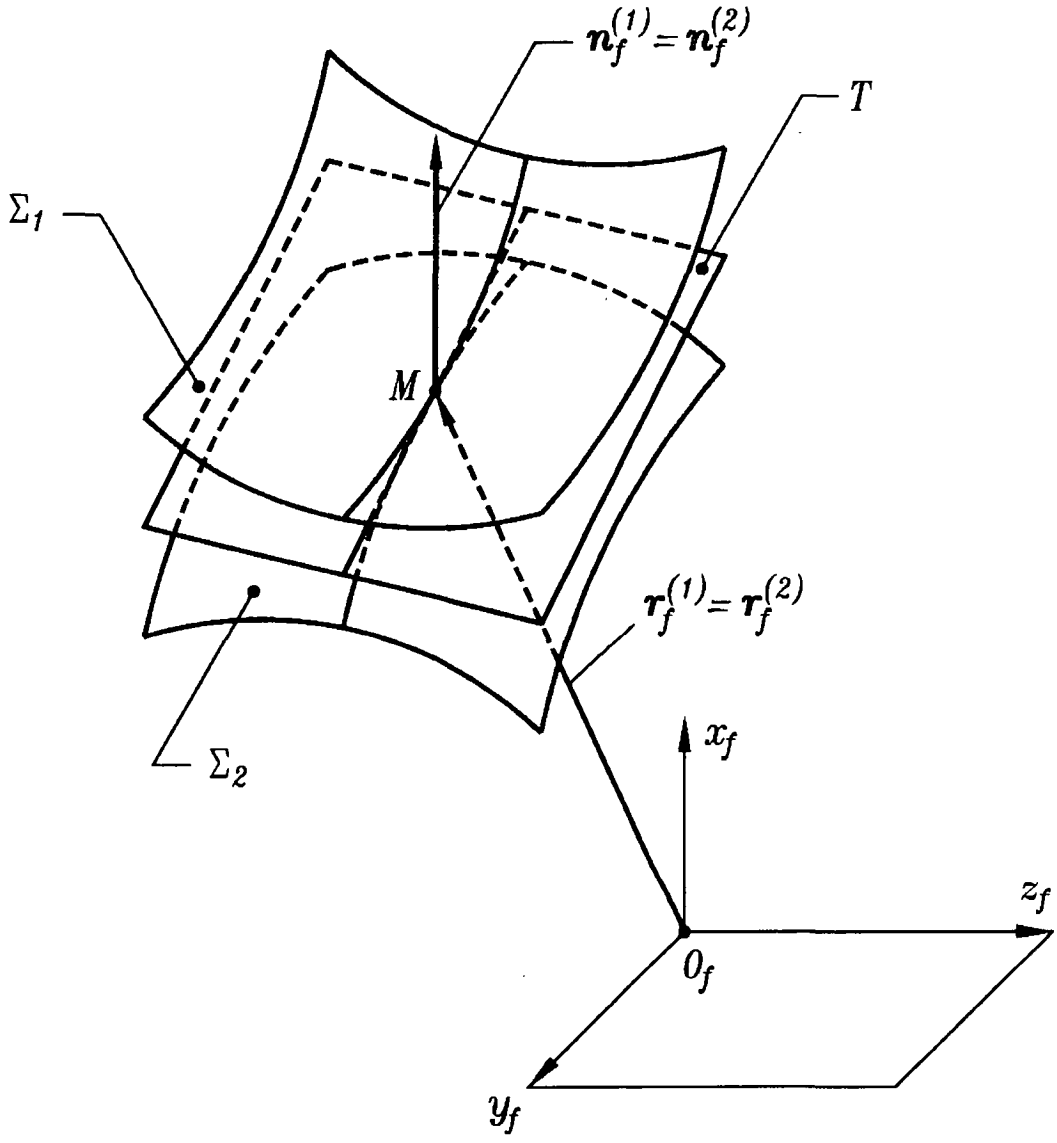

Figure 13: Tangency of contacting surfaces.

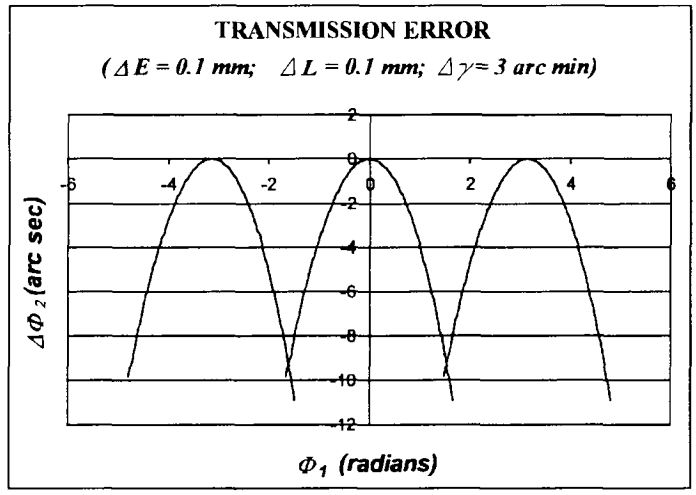

(a)

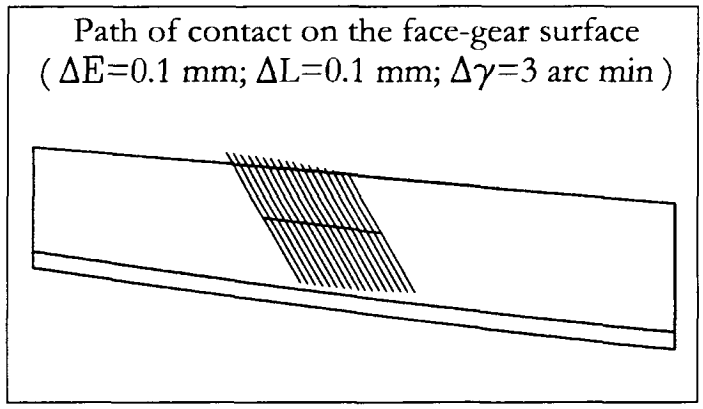

(b)

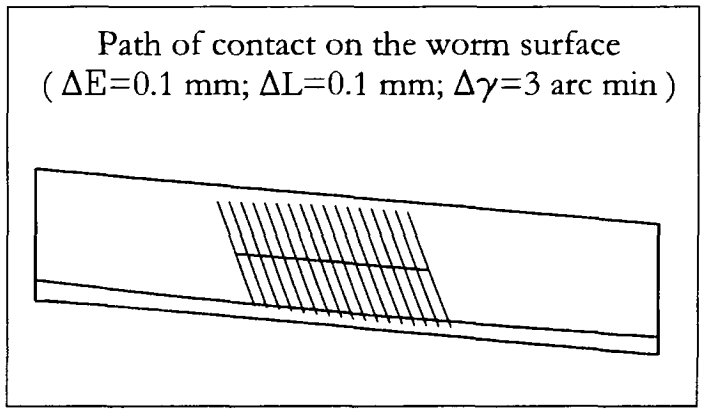

(c)

Figure 14: Output of TCA for a face gear drive with conical worm: (a) Transmissions errors with ΔE = 0.1 mm, ΔL = 0.1 mm, $\Delta\gamma$= 3 arc min; (b) path of contact on the face-gear surface with ΔE = 0.1 mm, ΔL = 0.1 mm, $\Delta\gamma$= 3 arc min; (c) path of contact on the worm surface with ΔE = 0.1 mm, ΔL = 0.1 mm, $\Delta\gamma$= 3 arc min.

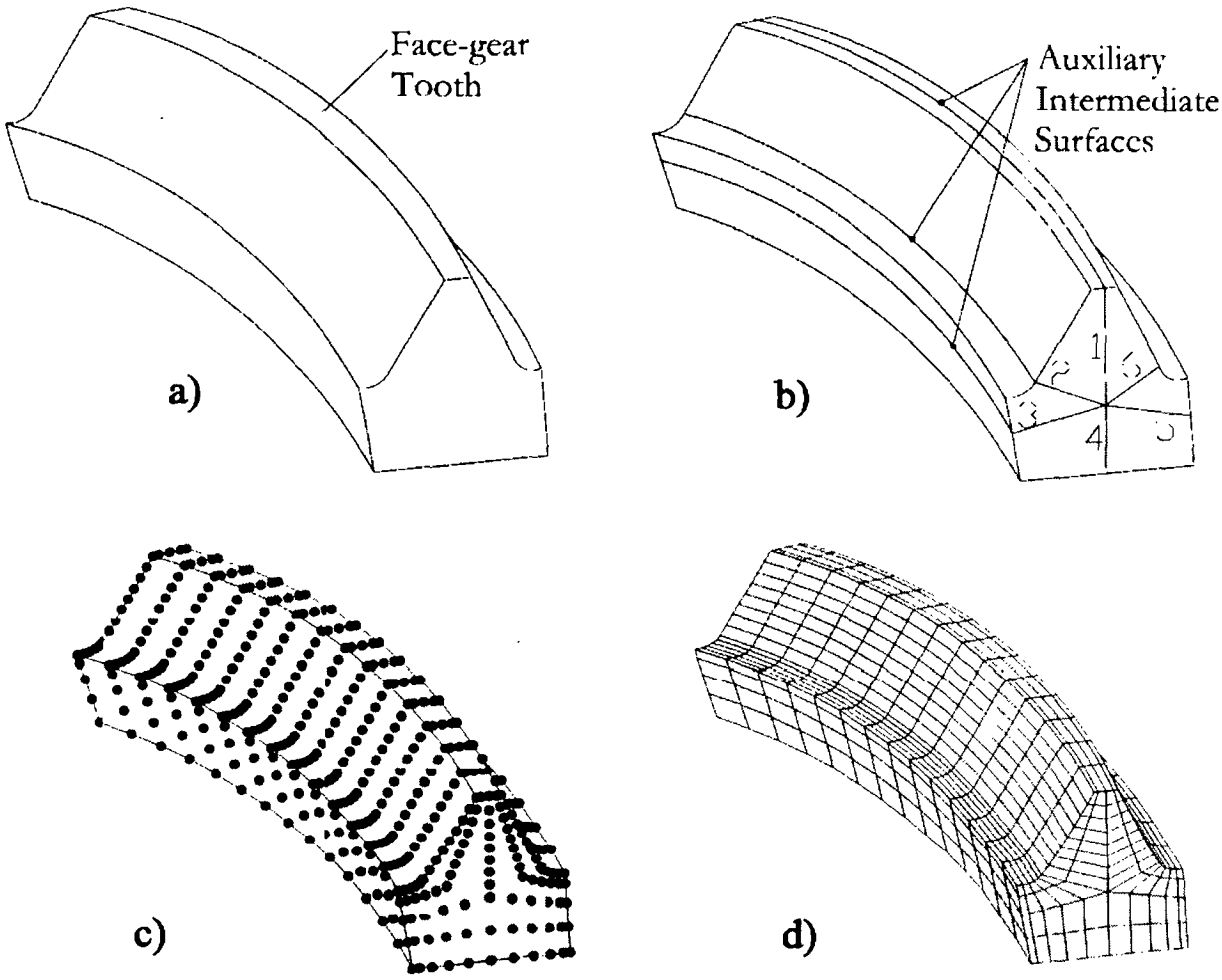

Figure 15: Illustration of: a) the volume of the designed body, b) auxiliary intermediate surfaces, c) determination of nodes for the whole volume, and d) discretization of the volume by finite elements.

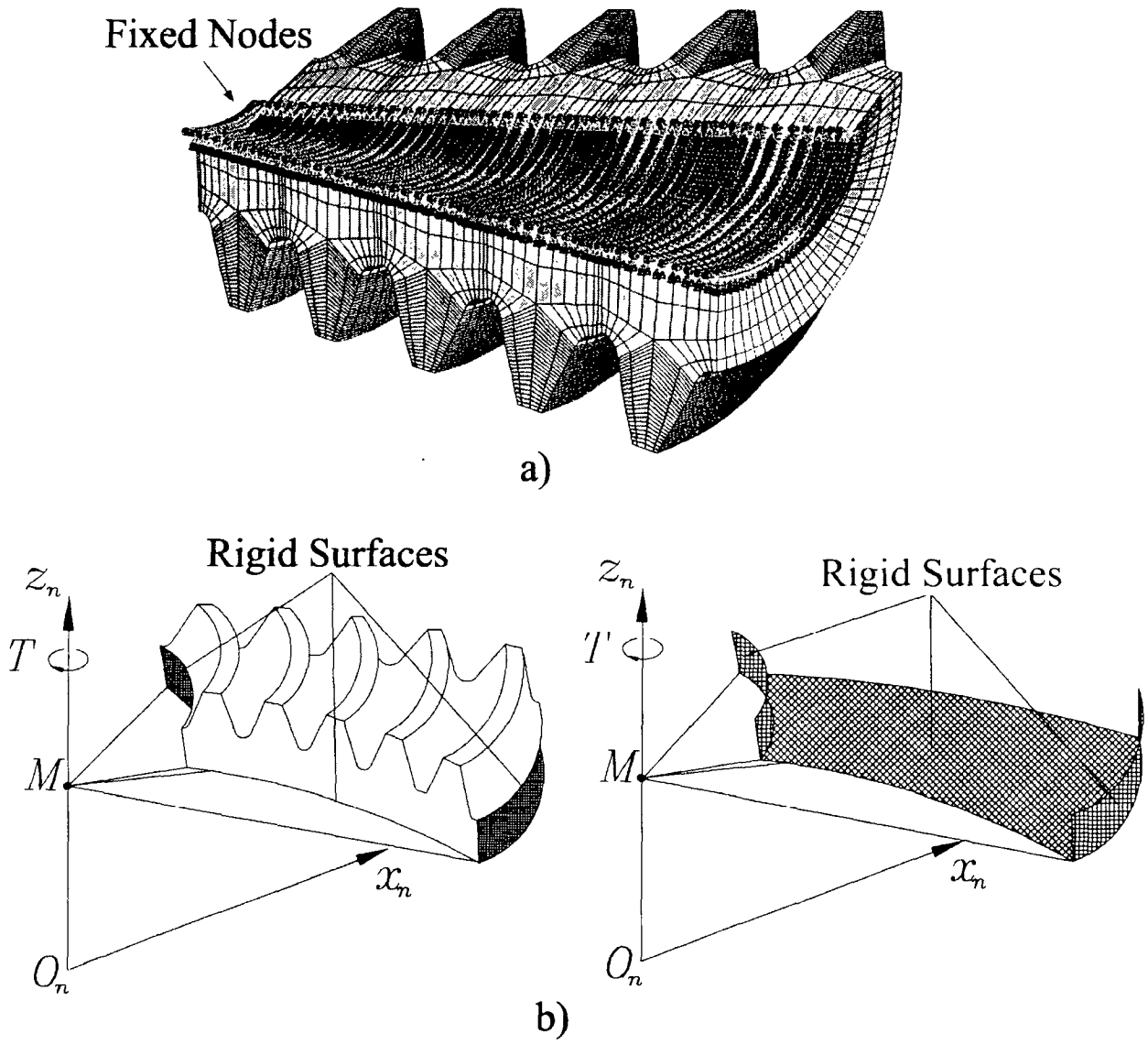

Figure 16: Schematic illustration of: a) boundary condition for the worm, and b) boundary conditions for the face-gear.

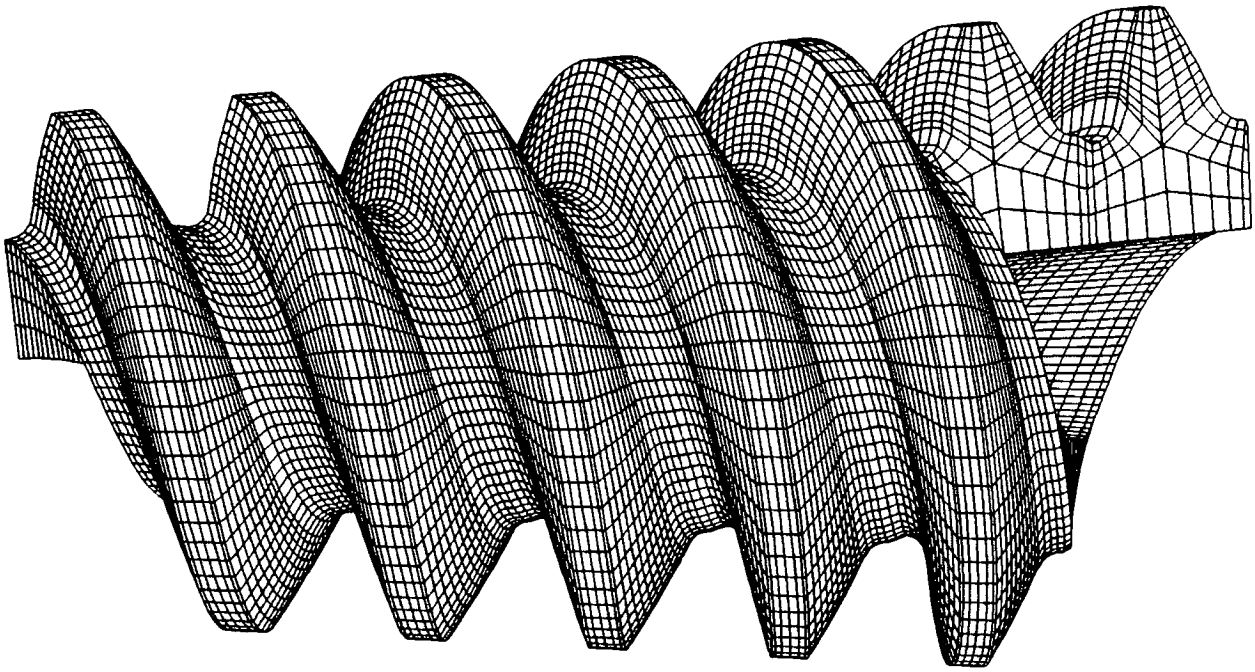

Figure 17: Finite element model of the whole worm.

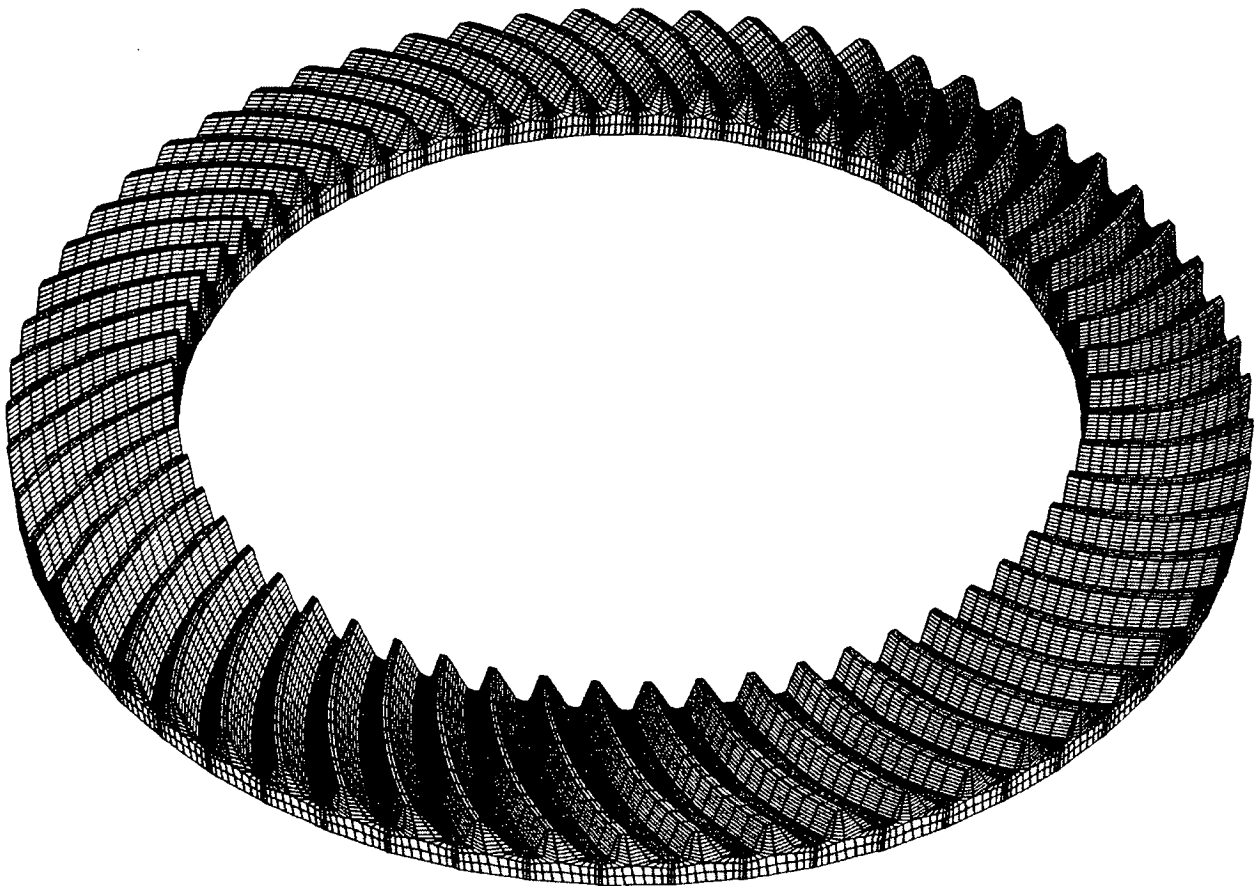

Figure 18: Finite element model of the whole face-gear.

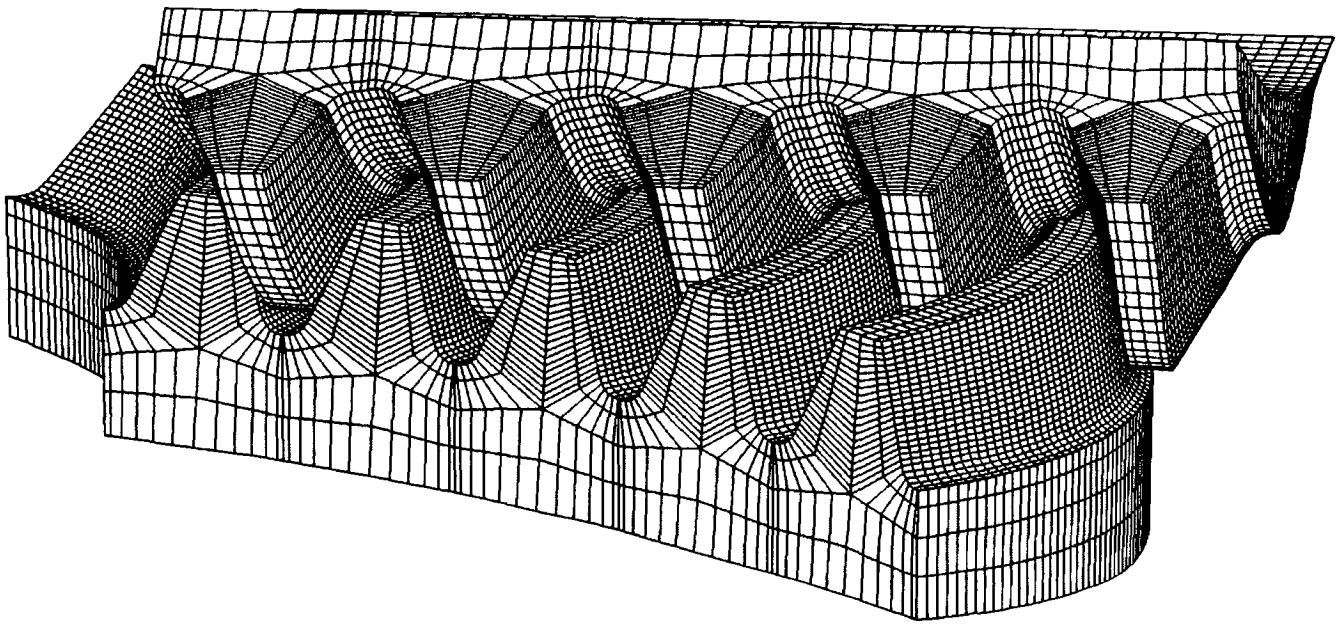

Figure 19: Face-gear drive with conical worm: finite element model of five teeth in mesh.

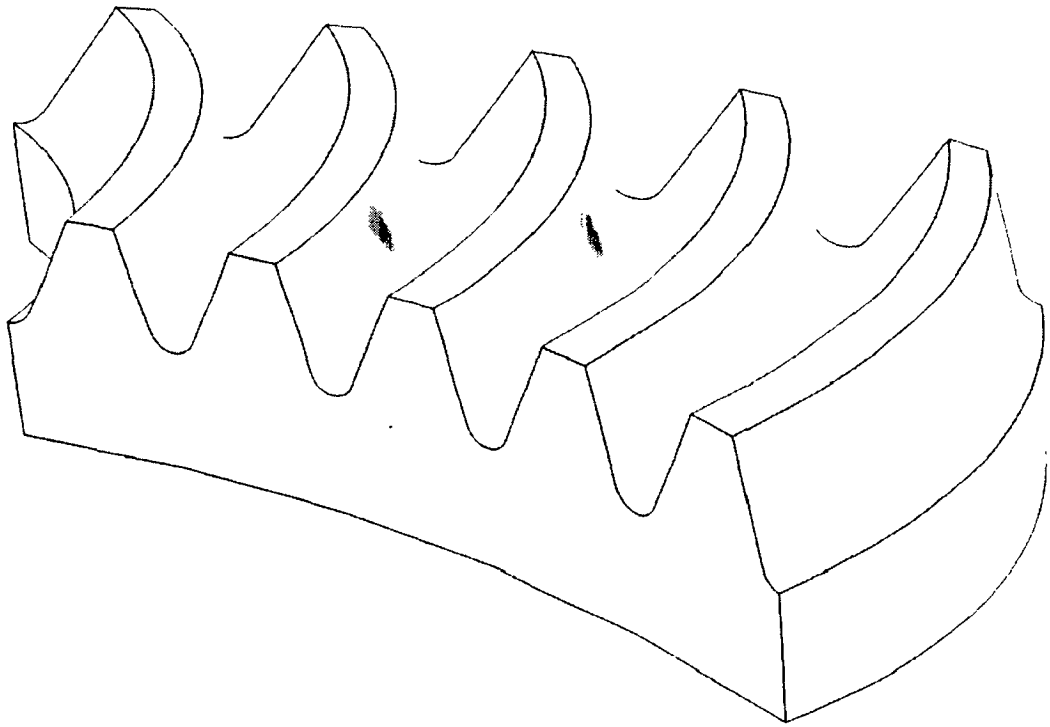

Figure 20: Face-gear drive with conical worm: bearing contact at the beginning of the cycle of meshing.

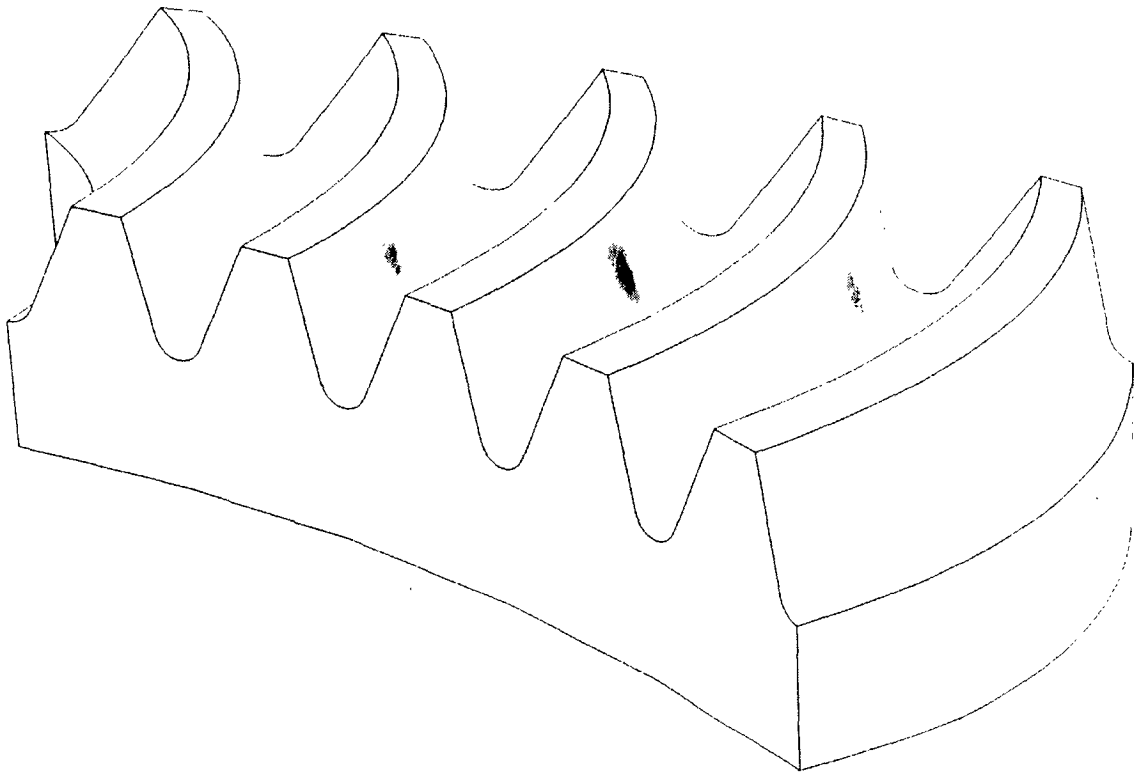

Figure 21: Face-gear drive with conical worm: bearing contact at the middle point of the cycle of meshing.

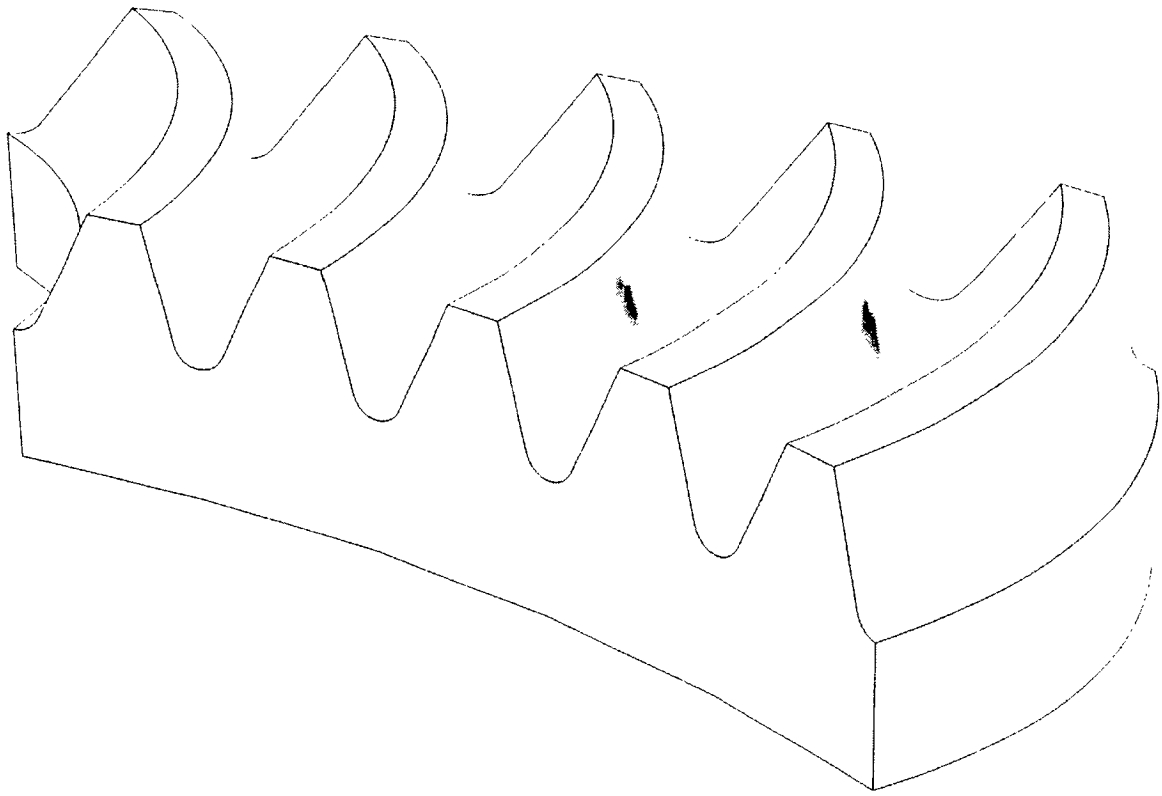

Figure 22: Face-gear drive with conical worm: bearing contact at the end of the cycle of meshing.

a)

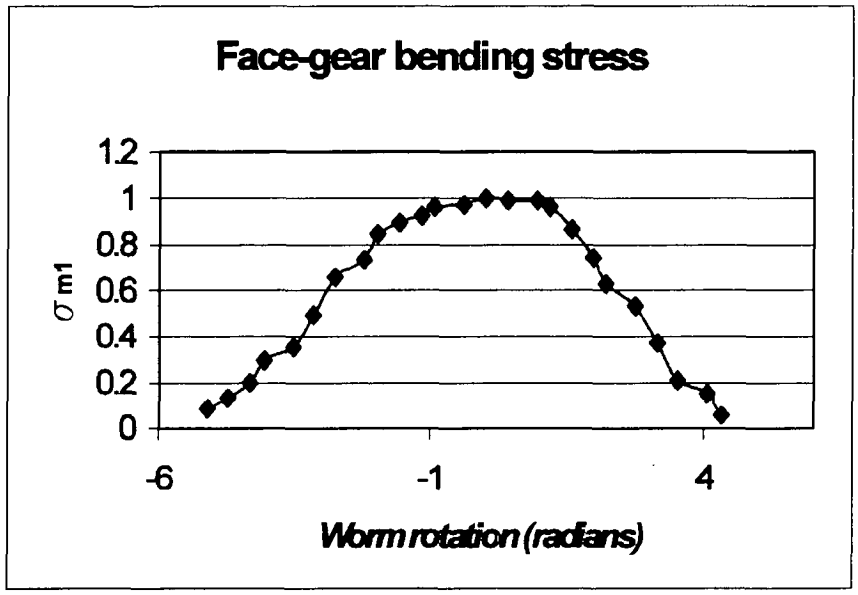

b)

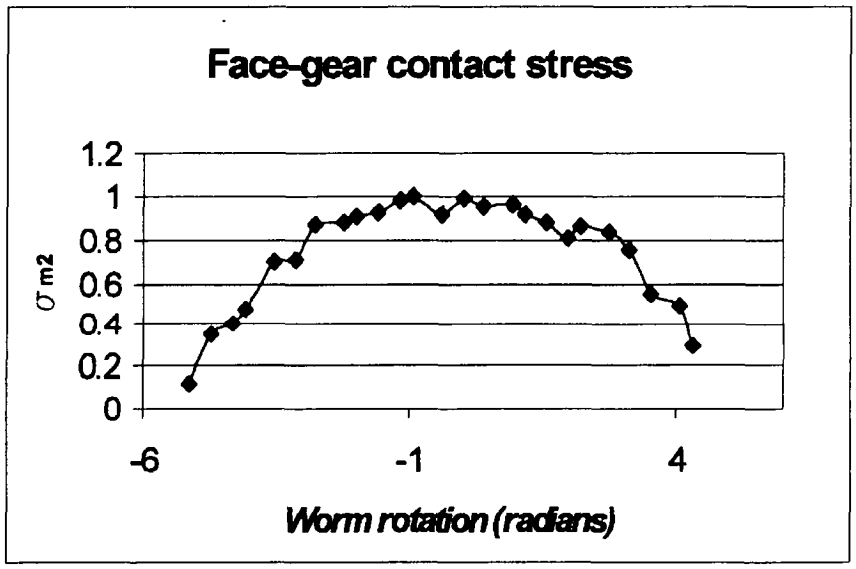

Figure 23: Face-gear drive with conical worm: a) Bending stress on the face-gear tooth in function of the pinion angle; b) Bending stress on the face-gear tooth in function of the pinion angle.

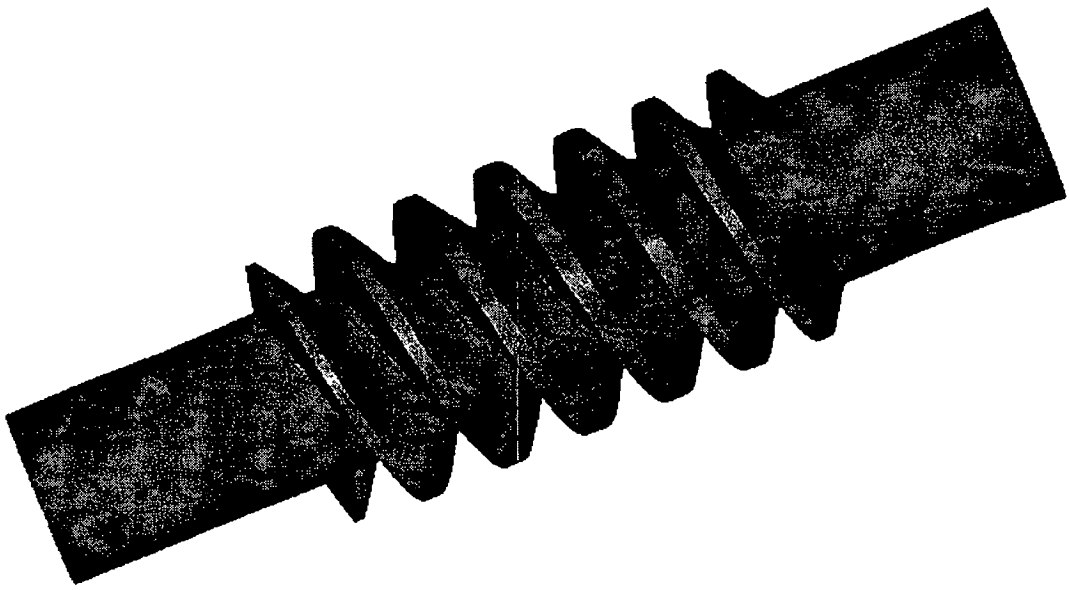

Figure 24: Cylindrical worm thread surfaces in 3D space.

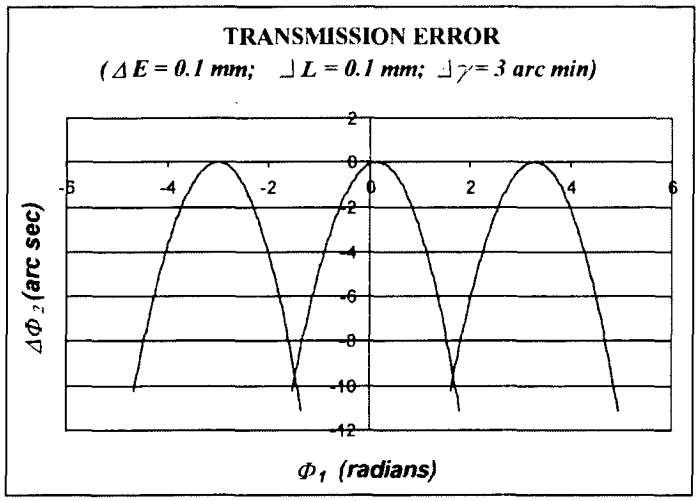

(a)

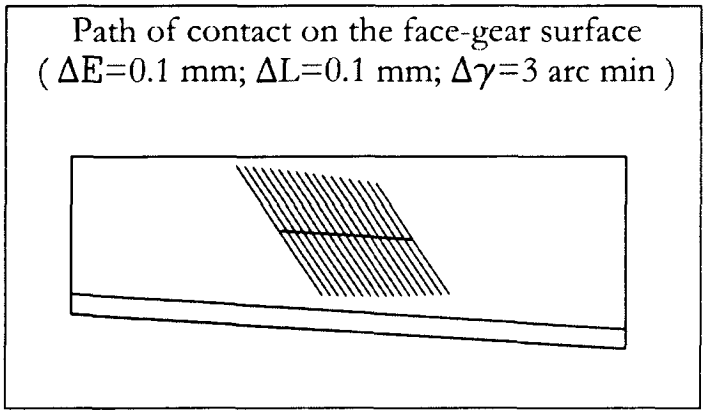

(b)

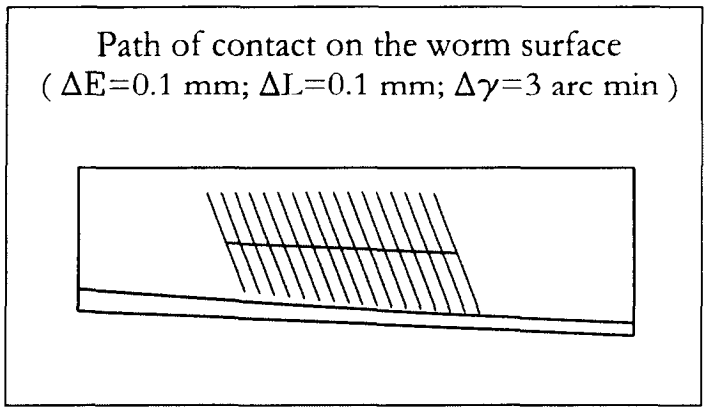

(c)

Figure 25: Output of TCA for a face gear drive with a cylindrical worm: (a) Transmission errors with ΔE = 0.1 mm, ΔL = 0.1 mm, $\Delta\gamma$= 3 arc min; (b) path of contact on the face-gear surface with ΔE = 0.1 mm, ΔL = 0.1 mm, $\Delta\gamma$= 3 arc min; (c) path of contact on the worm surface with ΔE = 0.1 mm, ΔL = 0.1 mm, $\Delta\gamma$= 3 arc min.

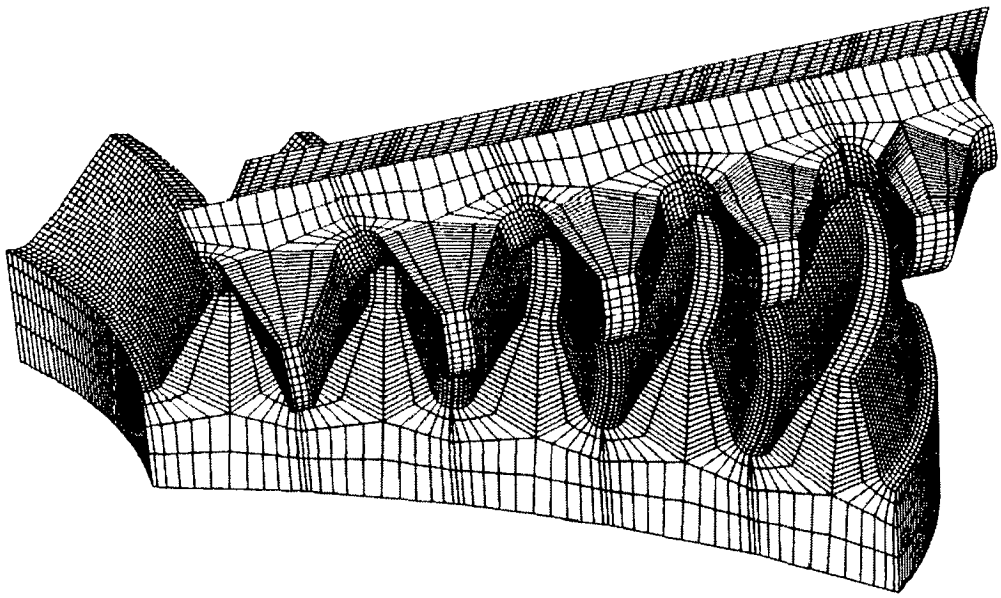

Figure 26: Face-gear drive with cylindrical worm: finite element model of five teeth in mesh.

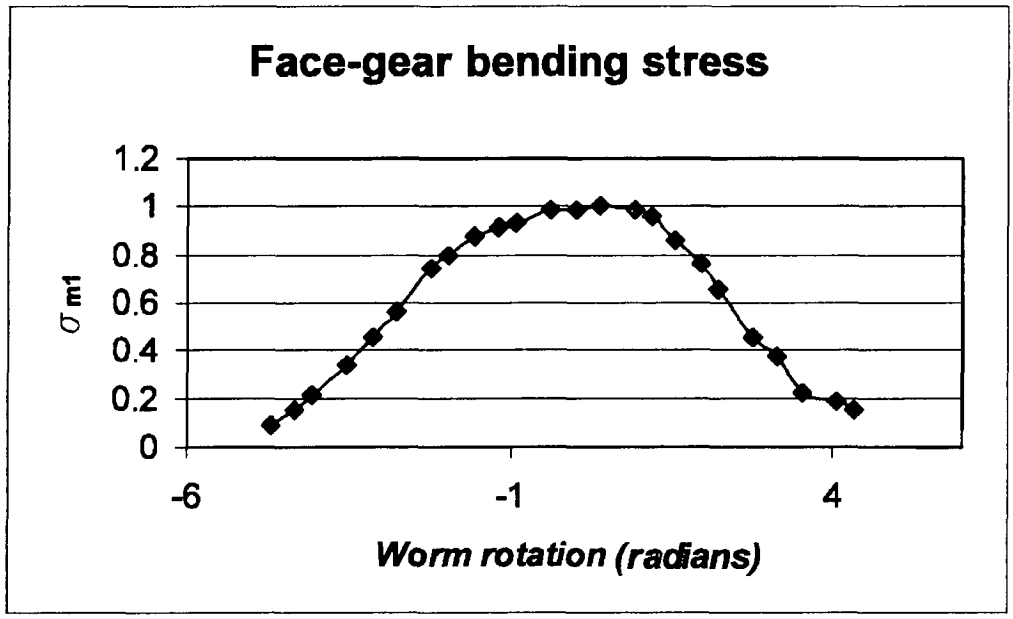

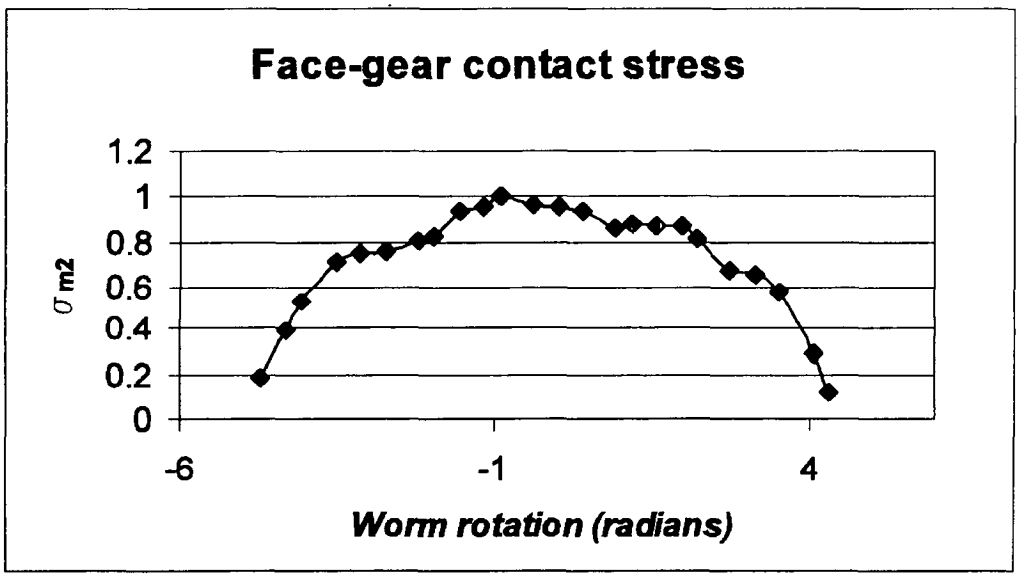

Figure 27: Face-gear drive with cylindrical worm: (a) Bending stress on the face-gear tooth in function of the pinion angle; (b) Bending stress on the face-gear tooth in function of the pinion angle.

REPORT DOCUMENTATION PAGE

Form Approved
OMB No. 0704-0188

1. AGENCY USE ONLY (*Leave blank*)	2. REPORT DATE	3. REPORT TYPE AND DATES COVERED
	November 2002	Final Contractor Report

4. TITLE AND SUBTITLE

New Geometry of Worm Face Gear Drives With Conical and Cylindrical Worms: Generation, Simulation of Meshing, and Stress Analysis

5. FUNDING NUMBERS

WU–722–90–06–00
NAG3–2450
1L162211A47A

6. AUTHOR(S)

Faydor L. Litvin, Alessandro Nava, Qi Fan, and Alfonso Fuentes

7. PERFORMING ORGANIZATION NAME(S) AND ADDRESS(ES)

University of Illinois at Chicago
Chiago, Illinois 60612

8. PERFORMING ORGANIZATION REPORT NUMBER

E–13577

9. SPONSORING/MONITORING AGENCY NAME(S) AND ADDRESS(ES)

National Aeronautics and Space Administration
Washington, DC 20546–0001
and
U.S. Army Research Laboratory
Adelphi, Maryland 20783–1145

10. SPONSORING/MONITORING AGENCY REPORT NUMBER

NASA CR—2002-211895
ARL–CR–0511

11. SUPPLEMENTARY NOTES

Project Manager, Robert F. Handschuh, U.S. Army Research Laboratory, Vehicle Technology Directorate, Structures and Acoustics Division, NASA Glenn Research Center, organization code 5950, 216–433–3969.

12a. DISTRIBUTION/AVAILABILITY STATEMENT

Unclassified - Unlimited
Subject Category: 37 Distribution: Nonstandard

Available electronically at http://gltrs.grc.nasa.gov

This publication is available from the NASA Center for AeroSpace Information, 301–621–0390.

12b. DISTRIBUTION CODE

13. ABSTRACT ***(Maximum 200 words)***

New geometry of face worm gear drives with conical and cylindrical worms is proposed. The generation of the face worm-gear is based on application of a tilted head-cutter (grinding tool) instead of application of a hob applied at present. The generation of a conjugated worm is based on application of a tilted head-cutter (grinding tool) as well. The bearing contact of the gear drive is localized and is oriented longitudinally. A predesigned parabolic function of transmission errors for reduction of noise and vibration is provided. The stress analysis of the gear drive is performed using a three-dimensional finite element analysis. The contacting model is automatically generated. The developed theory is illustrated with numerical examples.

14. SUBJECT TERMS	15. NUMBER OF PAGES
Gears; Transmissions	45
	16. PRICE CODE

17. SECURITY CLASSIFICATION OF REPORT	18. SECURITY CLASSIFICATION OF THIS PAGE	19. SECURITY CLASSIFICATION OF ABSTRACT	20. LIMITATION OF ABSTRACT
Unclassified	Unclassified	Unclassified	